

From the
Institut für Prophylaxe und Epidemiologie der Kreislaufkrankheiten (IPEK)
At the Klinikum der Ludwig-Maximilians-Universität München
Direktor: Univ.-Prof. Dr. med. Christian Weber



Dissertation zum Erwerb des
Doctor of Philosophy (Ph.D.)
an der Medizinischen Fakultät der
Ludwig-Maximilians-Universität zu München

**Co-stimulatory and epigenetic targets to
balance the T cell IFN- γ /
IL-4 ratio in atherosclerosis**

vorgelegt von:

Michael Wade Lacy
aus Lynchburg, Virginia, United States

2021

Mit Genehmigung der Medizinischen Fakultät der
Ludwig-Maximilians-Universität zu München

First supervisor: Prof. Dr. rer. nat. Jürgen Bernhagen

Second supervisor: Dr. rer. nat. Dorothee Atzler

Third supervisor: Prof. Dr. Axel Imhof

Dean: **Prof. Dr. med. Thomas Gudermann**

Date of Oral Defense: 9.12.21

Affidavit



Promotionsbüro
Medizinische Fakultät



Affidavit

Lacy, Michael

Surname, first name

Street

Zip code, town, country

I hereby declare, that the submitted thesis entitled:

Co-stimulatory and epigenetic targets to balance the T cell IFN- γ /IL-4 ratio in atherosclerosis

is my own work. I have only used the sources indicated and have not made unauthorised use of services of a third party. Where the work of others has been quoted or reproduced, the source is always given.

I further declare that the submitted thesis or parts thereof have not been presented as part of an examination degree to any other university.

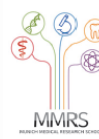
Munich, 10.12.21
place, date

Michael Lacy
Signature doctoral candidate

Confirmation of congruency



Promotionsbüro
Medizinische Fakultät



**Confirmation of congruency between printed and electronic version of
the doctoral thesis**

Lacy, Michael

Surname, first name

Street

Zip code, town, country

I hereby declare, that the submitted thesis entitled:

Co-stimulatory and epigenetic targets to balance the T cell IFN- γ /IL-4 ratio in atherosclerosis

is congruent with the printed version both in content and format.

Munich, 10.12.21

place, date

Michael Lacy
Signature doctoral candidate

Table of Contents

Affidavit	3
Confirmation of congruency	4
Table of Contents	5
List of abbreviations	7
List of publications	9
1. Publications included in this dissertation.....	9
2. Additional publications not included in this dissertation.....	10
1. Contribution to Publications.....	11
1. Contribution to Paper I: Cell-specific and divergent roles of the CD40L-CD40 axis in atherosclerotic vascular disease	11
2. Contribution to Paper II: Glucocorticoid-induced tumour necrosis factor receptor family-related protein (GITR) drives atherosclerosis in mice and is associated with an unstable plaque phenotype and cerebrovascular events in humans	12
3. Contribution to paper III (Appendix A): Interactions between dyslipidemia and the immune system and their relevance as putative therapeutic targets in atherosclerosis.	13
4. Contribution to paper IV (Appendix B): T-cell EZH2 regulates type II cytokine production: a potential therapeutic target in atherosclerosis.....	13
2. Introductory summary.....	14
2.1. Atherosclerosis	14
2.2. The role of T cells in atherosclerosis.....	16
2.3. T cell activation and differentiation	20
2.4. Rationale.....	23
References	25
3. Paper I: Cell-specific and divergent roles of the CD40L-CD40 axis in atherosclerotic vascular disease.....	29
4. Paper II: Glucocorticoid-induced tumour necrosis factor receptor family-related protein (GITR) drives atherosclerosis in mice and is associated with an unstable plaque phenotype and cerebrovascular events in humans	30
Appendix A: Paper III: Interactions between dyslipidemia and the immune system and their relevance as putative therapeutic targets in atherosclerosis	31

Appendix B: Paper IV: T-cell EZH2 regulates type II cytokine production: a potential therapeutic target in atherosclerosis.....	32
Acknowledgements.....	88

List of abbreviations

$\alpha\beta$ T cell	Alpha beta (Conventional) T cell
alpha-GalCer	Alpha-galactosylceramide
AP-1	Activator protein 1
APC	Antigen presenting cell
ApoE	Apolipoprotein E
CANTOS	Canakinumab Anti-Inflammatory Thrombosis Outcome Study
CCL2	C-C-Motif chemokine ligand 2
CCR5	C-C Motif chemokine receptor 5
CLTA4	Cytotoxic T-lymphocyte-associated protein 4
CD	Cluster of differentiation
CD40L	CD40 ligand
CIRT	Cardiovascular Inflammation Reduction Trial
COLCOT	Colchicine Cardiovascular Outcomes Trial
CXCR3	C-X-C motif chemokine receptor 3
CyTOF	Mass cytometry by time of flight
EZH2	Enhancer of zeste homolog 2
FACs	Fluorescence-activated cell sorting
FoxP3	Forkhead box P3
$\gamma\delta$ T cell	Gamma delta T cell
GATA3	GATA binding protein 3
GITR	Glucocorticoid-induced tumor necrosis factor receptor
H3K4me3	Histone 3 lysine 4 trimethylation
H3K27me3	Histone 3 lysine 27 trimethylation
hsCRP	High sensitivity C reactive protein
IgSF	Immunoglobulin superfamily
IL	Interleukin
IL-4R	Interleukin-4 receptor
IFN- γ	Interferon-gamma

LDL	Low density lipoprotein
LDLr	Low density lipoprotein receptor
LoDoCo2	Low-Dose Colchicine Trial
MHC	Major histocompatibility complex
NFAT	Nuclear factor of activated T cells
NKT	Natural killer T cell
oxLDL	Oxidized low density lipoprotein
PLZF	Promyelocytic leukaemia zinc finger
RNA	Ribonucleic acid
ROR γ t	RAR-related orphan receptor gamma
scRNA-seq	Single cell RNA sequencing
T-bet	T-box transcription factor
TGF- β	Transforming growth factor beta
Th	T helper cell
TNFRSF	Tumor necrosis factor receptor superfamily
Treg	T regulatory cell

The results of this work have been or will be published in:

• **Paper I**

Lacy, M.*, Bürger, C.*, Shami, A.*, Ahmadsei, M., Winkels, H., Nitz, K., van Tiel, C. M., Seijkens, T. T. P., Kusters, P. J. H., Karshovka, E., Prange, K. H. M., Wu, Y., Brouns, S. L. N., Unterlugauer, S., Kuijpers, M. J. E., Reiche, M. E., Steffens, S., Edsfeldt, A., Megens, R. T. A., Heemskerk, J.W.M., Gonclaves, I., Weber, C., Gerdes, N.#, Atzler, D.#, Lutgens, E.# (2021). Cell-specific and divergent roles of the CD40L-CD40 axis in atherosclerotic vascular disease. *Nature Communications*, 12(1), 1–12. <https://doi.org/10.1038/s41467-021-23909-z>

• **Paper II**

Shami, A.* , Atzler, D.* , Bosmans, L. A., Winkels, H., Meiler, S., **Lacy, M.**, van Tiel, C., Megens, R. T., Nitz, K., Baardman, J., Kusters, P., Seijkens, T., Buerger, C., Janjic, A., Riccardi, C., Edsfeldt, A., Monaco, C., Daemen, M., de Winther, M. P. J., Nilson, J., Weber, C., Gerdes, N., Gonclaves, I.#, Lutgens, E.# (2020). Glucocorticoid-induced tumour necrosis factor receptor family-related protein (GITR) drives atherosclerosis in mice and is associated with an unstable plaque phenotype and cerebrovascular events in humans. *European Heart Journal*, 41(31), 2938–2948. <https://doi.org/10.1093/eurheartj/ehaa484>

• **Paper III**

Lacy, M., Atzler, D., Liu, R., de Winther, M., Weber, C., & Lutgens, E. (2019). Interactions between dyslipidemia and the immune system and their relevance as putative therapeutic targets in atherosclerosis. *Pharmacology and Therapeutics*, 193, 50–62. <https://doi.org/10.1016/j.pharmthera.2018.08.012>

• **Paper IV**

Lacy, M., Janjic, A., Nitz, K., Bonfiglio, C., Kumkum, M., Wu, Y., Wange, L.E., Santovito, D., Unterlugauer, S., Bosmans, L.A., Venkatasubramini, A., Imhof, A., Maegdefessel, L., Enard, W., Weber, C., de Winther, M.P.J. Atzler, D.#, Lutgens, E.# T-cell EZH2 regulates type II cytokine production: a potential therapeutic target in atherosclerosis. *In preparation*

Additional publications not included in this work:

Nitz, K.* , **Lacy, M.***, Bianchini, M., Wu, Y., Preischl, C., Aslani, M., Li, Y., Forne, I., Ammar, C., Janjic, A., Mohanta, S., Duchene, J., Megens, R.T.A., Schwedhelm, E., Huveneers, S., Zimmer, R., Imhof, A., Weber, C., Lutgens, E., Atzler, D. The amino acid homoarginine inhibits atherogenesis by modulating T-cell function. *In preparation*

Gencer, S.* , **Lacy, M.***, Atzler, D., Van Der Vorst, E. P. C., Döring, Y., & Weber, C. (2020). Immunoinflammatory, Thrombohaemostatic, and Cardiovascular Mechanisms in COVID-19. *Thrombosis and Haemostasis*, 120(12), 1629–1641. <https://doi.org/10.1055/s-0040-1718735>

Bianchini, M., Duchêne, J., Santovito, D., Schloss, M. J., Evrard, M., Winkels, H., Aslani, M., Mohanta, S. K., Horckmans, M., Blanchet, X., **Lacy, M.**, Von Hundelshausen, P., Atzler, D., Habenicht, A., Gerdes, N., Pelisek, J., Ng, L. G., Steffens, S., Weber, C., & Megens, R. T. A. (2019). PD-L1 expression on nonclassical monocytes reveals their origin and immunoregulatory function. *Science Immunology*, 4(36). <https://doi.org/10.1126/sciimmunol.aar3054>

Nitz, K., **Lacy, M.**, & Atzler, D. (2019). Amino acids and their metabolism in atherosclerosis. *Arteriosclerosis, Thrombosis, and Vascular Biology*, 39(3), 319–330. <https://doi.org/10.1161/ATVBAHA.118.311572>

Lacy, M.*, Kontos, C.* , Brandhofer, M.* , Hille, K., Gröning, S., Sinitski, D., Bourilhon, P., Rosenberg, E., Krammer, C., Thavayogarajah, T., Pantouris, G., Bakou, M., Weber, C., Lolis, E., Bernhagen, J.# , Kapurniotu, A.# (2018). Identification of an Arg-Leu-Arg tripeptide that contributes to the binding interface between the cytokine MIF and the chemokine receptor CXCR4. *Scientific Reports*, 8(1), 1–17. <https://doi.org/10.1038/s41598-018-23554-5>

Francis, S., Katz, J., Fanning, K.D., Harris, K.A., Nicholas, B.D., **Lacy, M.**, Pagana, J., Agris, P.F., Shin, J.B. (2013). A Novel Role of Cytosolic Protein Synthesis Inhibition in Aminoglycoside Ototoxicity. *Journal of Neuroscience*, 33(7), 3079-3093. <https://doi.org/10.1523/JNEUROSCI.3430-12.2013>

* denotes shared first authorship

denotes shared last authorship

1. Contribution to Publications

1. Contribution to Paper I: Cell-specific and divergent roles of the CD40L-CD40 axis in atherosclerotic vascular disease

Lacy, Bürger, and Shami share co-first authorship of this publication. Lacy and Bürger both worked extensively on the three mouse models described within the paper while Shami worked solely on the human cohort (Paper section: sCD40L and sCD40 levels correlate with IFN- γ in human plasma and atherosclerotic plaques). Within the murine studies, Lacy confirmed the cell-specific deletions (Supplemental Figures 1 and 2) while Bürger provided the preliminary studies assessing the atherosclerotic burden of the cell-specific CD40 and CD40L-deficient mice. Together with Ahmadsei, Heemskerk, and Gerdes, Bürger phenotyped the platelet CD40L knockout model as described in Figure 2. Lacy continued follow-up studies on the T-cell CD40L knockout model to help characterize the atherosclerotic lesions, and specifically worked to assess the stability of the plaques using a Virmani classification as well as the immunocytochemical and histological stainings as described in Figure 1. Furthermore, to uncover the underlying mechanism, Lacy observed the reduction *IFN- γ* mRNA transcripts within the aorta, which led to his follow-up studies characterizing T helper (Th) and T regulatory cell populations as described in Figure 3. After he observed the reduction in Th1 cells, Lacy performed the DC-T cell co-culture to confirm lower IFN- γ production in the absence of CD40-CD40L signaling as described in Figure 5. Together with Atzler and Lutgens, Lacy wrote the manuscript.

2. Contribution to Paper II: Glucocorticoid-induced tumour necrosis factor receptor family-related protein (GITR) drives atherosclerosis in mice and is associated with an unstable plaque phenotype and cerebrovascular events in humans

Lacy is a co-author of this publication. Lacy worked extensively on the murine GITR knock-out mice while maintaining the mouse strain in Munich. To help establish the role of hematopoietic GITR in atherosclerosis, Lacy performed a bone marrow transplant together with Seijkens. As lesional macrophages were decreased in GITR-deficient mice, Lacy isolated classical and non-classical monocytes and subsequently created bulk RNA sequencing libraries together with Janjic. Considering pathway analysis revealed potential migratory effects, Lacy performed *ex vivo* leukocyte adhesion assays together with Atzler and Megens using bone marrow-derived leukocytes and carotid arteries of GITR wild type and deficient mice as described in Figure 5. Finally, Lacy characterized expression of adhesion molecules in classical and non-classical monocytes as well as granulocytes via flow cytometry.

3. Contribution to paper III (Appendix A): Interactions between dyslipidemia and the immune system and their relevance as putative therapeutic targets in atherosclerosis.

Lacy is the sole first author of this review. Lacy wrote the manuscript, which Atzler and Lutgens later edited. Together with Liu, Lacy created the figures. This additional contribution to the dissertation provides additional background for the rationale of the studies.

4. Contribution to paper IV (Appendix B): T-cell EZH2 regulates type II cytokine production: a potential therapeutic target in atherosclerosis

Lacy is the sole first author of this manuscript. Lacy worked extensively on the murine studies of the CD4⁺ and CD8⁺ EZH2 deficient mice. Lacy confirmed both knockout models, and Venkatasubramini completed the mass spectrometry of isolated histones. Lacy completed the atherosclerosis studies for both mouse strains as well as helped phenotype the lesions. Lacy isolated cells prior to library creation, Janjic and Wange helped create both bulk and single cell RNA sequencing libraries, and Lacy analyzed the data. Flow cytometric and qPCR analysis was performed by Lacy. Together with de Winther, Atzler, and Lutgens, Lacy designed the study. Atzler, Lutgens, and Lacy wrote the manuscript. This additional contribution to the dissertation is unpublished, but provides additional insight about Lacy's scientific work during his PhD studies.

2. Introductory summary

2.1. Atherosclerosis

Atherosclerosis, which is the major underlying pathology of cardiovascular disease (CVD), is a dyslipidemia-driven, chronic inflammatory disorder¹. The subsequent clinical manifestations of CVD, including myocardial infarction and stroke, remain a leading cause of death worldwide².

During the initiation of atherosclerotic plaque development and its ensuing progression, the interplay between lipids and immune cells help promote lesion growth and vascular dysfunction³. Within the vessel, lipids tend to accumulate in the intimal layer of vessels near areas of disturbed blood flow ultimately activating endothelial cells (ECs) that up-regulate cell adhesion molecules⁴. Circulating leukocytes, in turn, are able to attach to the vessel wall and migrate towards the deposited lipids in the intima layer forming initial lesions. Early immune responders such as monocytes transmigrate in order to mediate lipoprotein uptake as lesional macrophages. The inflamed intima region results in a multitude of secreted chemokines, which attracts further immune cells including both innate and adaptive immune cell subsets such as neutrophils and T cells⁵. Therefore, in order to begin to treat atherosclerosis, we must first understand the diverse cellular makeup responsible for the inflammation and ultimately the disease.

In the past, histological and immunohistochemical (IHC) evidence was incorporated to classify plaque-resident leukocytes; however, recent studies have begun utilizing single cell RNA –sequencing (scRNA-seq) and mass cytometry by time of flight (CyTOF) technologies to unravel the exact cellular components of both mouse and human atherosclerotic plaques. Although these novel technologies are more sensitive and have greatly expanded our understanding of plaques, they have not completely resolved questions concerning cellular heterogeneity. This is especially evident as the two identification systems show noted discrepancies in the relative abundance of different cell types. For example, traditional imaging studies report lesional macrophage content to represent a majority of lesional cells⁶⁻⁸. On the other hand, single cell methods have identified T cells rather than macrophages as the major component of human atherosclerotic plaques, specifically Fernandez et al used CyTOF to identify T cells as 65% of all immune cells while

scRNA-seq from Depuydt et al identified roughly 52% of all lesional immune cells as T cells^{9,10}. Tissue disruption methods used to prepare single cell suspensions, such as enzymatic digestion and fluorescence-activated cell sorting (FACs), may account for discrepancies in relative cell numbers as more fragile cells, such as foamy, lipid-loaded macrophages, may be susceptible to mechanical stress induced death¹¹. Additionally, traditional methods lack the ability to differentiate between subtypes of lesional cells which require multi-marker analysis, and thus may result in the observed differences between methods¹².

While there are limitations to both single cell methods and imaging studies, single cell methods are quickly becoming a gold standard as transcriptomic data has allowed for deeper phenotyping of lesional immune cells. In particular, the cell heterogeneity of T cells has greatly expanded to include various differentiation states such as naïve, effector, and antigen-specific cells within the atherosclerotic mouse aortas¹³. In humans, distinct T cell activation and differentiation phenotypes were observed in carotid artery plaques from patients with recent ischemic attacks compared to asymptomatic patients⁹. Therefore, targeting T cell activation and differentiation pathways represents an attractive immunotherapy alternative to traditional lipid lowering therapies.

In the past, lipid lowering therapies such as statins were identified as the gold standard to treat atherosclerosis; however, recent evidence from several clinical trials has demonstrated that underlying inflammatory processes in atherosclerosis can be targeted in addition to further reduce risk. The first proof-of-concept cardiovascular immunotherapy in humans was described in the *Canakinumab Anti-Inflammatory Thrombosis Outcome Study* (CANTOS) trial¹⁴. Here, inhibition of the interleukin (IL)-1 β pathway, a well-established pro-inflammatory cytokine¹⁵, reduced the risk of cardiovascular events and cancer mortality in high risk patients who had previously suffered a myocardial infarction and continued to present residual inflammation, which was determined by a high sensitivity C reactive protein (hsCRP) measurement above 2 mg/L¹⁴. It is important to note, however, that while IL-1 β blockage using canakinumab reduced cardiovascular events, it had clear shortcomings in limiting mortality from cardiovascular events while increasing the risk of fatal infections. Shortly thereafter, however, the *Cardiovascular Inflammation Reduction Trial* (CIRT) failed to reduce cardiovascular risk in a similar patient setting. Within the CIRT trial, patients received a low dose of methotrexate, which is well-established as

non-specific anti-inflammatory agent¹⁶. While the outcomes of these two trials appear to be opposite, together they indicated that anti-inflammatory treatments likely need to be targeted in order to affect cardiovascular outcomes.

To further understand the role of inflammation in the context of atherosclerosis and its subsequent clinical manifestations, two additional clinical trials, namely the *Colchicine Cardiovascular Outcomes Trial* (COLCOT)¹⁷ and *Low-Dose Colchicine Trial* (LoDoCo2)¹⁸, investigated the role of an additional anti-inflammatory agent called colchicine. Mechanistically, colchicine functions more broadly by affecting tubulin polymerization¹⁹ and cell chemotaxis²⁰, which makes it more similar to methotrexate rather than to the selective inhibition observed with canakinumab. However, unlike methotrexate, colchicine treatment was able to lower the risk of cardiovascular events in both trials^{17,18}. Understanding the differing outcomes observed in the CIRT trial compared to the COLCOT and LoDoCo2 trials mandates for further development of specific effective anti-inflammatory agents to treat atherosclerosis. Therefore, targeting the underlying inflammatory processes including T cell responses during plaque progression may open new therapeutic avenues.

2.2. The role of T cells in atherosclerosis

The primary T cell subsets studied during the progression of atherosclerosis include Cluster of differentiation 4 (CD4⁺), CD8⁺, natural killer (NKT), and gamma delta ($\gamma\delta$) T cells. To dissect the role of these different T cells in atherosclerosis, genetic knockout models have been generated using T cell-specific genes backcrossed to hyperlipidemic mice, such as Apolipoprotein E-deficient (*ApoE*^{-/-}) or Low density lipoprotein receptor-deficient (*LDLR*^{-/-}) mice.

Within atherosclerotic lesions, CD4⁺ cells are the most well characterized T cell subset; however, CD4⁺ T cells display a wide range of both pro-atherogenic and anti-atherogenic phenotypes as well as subsets which remain controversial (Figure 1A)²¹. Following antigen presentation, CD4⁺ T cells can differentiate into distinct helper cells, including T helper (Th) 1, 2, and 17, or regulatory T (Treg) cell subsets in addition to other less well characterized cell types. Each subset can be identified by lineage specific transcription factors as well as cytokine profiles. Th1 cells are associated with T-box transcription factor (T-bet) and interferon-gamma (IFN- γ) expression while Tregs are linked to forkhead box

P3 (FoxP3) as well as transforming growth factor beta (TGF- β) and IL-10 expression. On the other hand, Th2 cells are associated with GATA binding protein 3 (GATA3) and IL-4 while Th17 cells are associated with RAR-related orphan receptor-gamma (ROR γ t) and IL-17²².

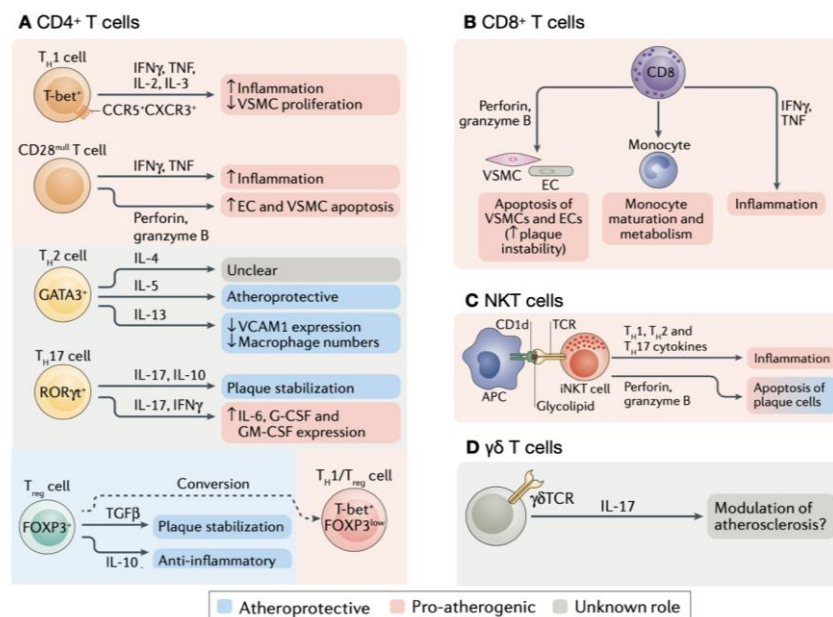


Figure 1: T cell subsets in atherosclerosis. (A) Th1 and CD28^{null} CD4⁺ T cell play pro-atherogenic roles in atherosclerosis through secretion of cytokines like interferon-gamma (IFN- γ), which affects vascular smooth muscle cells (VSMCs). The role of CD4⁺ Th2 and Th17 cells remains unclear as their signature cytokines, interleukin(IL-4 and IL-17 respectively), play differing roles in the context of atherosclerosis. T regulatory (Treg) cells are the clear atheroprotective CD4⁺ subset; however, they may convert to a pro-atherogenic Th1/Treg phenotype. (B) CD8⁺ T cells are thought of as pro-atherogenic cells as they can secrete molecules such as perforin and granzyme B that increase plaque instability through apoptosis of VSMCs and they also secrete pro-inflammatory cytokines like IFN- γ . These cells have also been linked to monocyte and macrophage maturation. (C) Natural killer T (NKT) cells are activated through an interaction between their T cell receptor (TCR) and the MHC-I-like molecule, CD1d. After activation, they secrete a variety of T helper (Th) cytokines as well as cytotoxic molecules, which may increase inflammation and apoptosis within plaques. (D) The role of gamma delta ($\gamma\delta$) T cells remains unclear; however, after activation they produce IL-17, which may affect atherosclerotic lesions in a manner similar to Th17 cells. Modified from Saigusa, Winkels, and Ley (2020)²¹. Reprinted with permission from Springer Nature (License #5140831217395).

Of those subsets, Th1 and Tregs appear to have opposing inflammatory and suppressive capacities in the context of atherosclerosis, respectively. Using a double *ApoE^{-/-}Tbet^{-/-}* knockout model, Buono et al were able to show a reduced Th1 response was associated with reduced plaque burden²³. Genetic deficiency of *IFN-γ* also led to a reduction in atherosclerosis, but in a gender-specific manner that only applied to male mice²⁴. In a separate study, injection of exogenous IFN-γ resulted in a two-fold increase in lesion size further cementing the pro-atherogenic role of Th1 cells²⁵. In human plaques, symptomatic patients have an enriched Th1 phenotype which express C-C motif chemokine receptor 5 (CCR5) and C-X-C motif chemokine receptor 3 (CXCR3) compared to asymptomatic patients⁹. In principle, Th1 cells may migrate through CCR5 and CXCR3 towards the inflamed intima, and their IFN-γ expression can erode plaque stability by inhibiting smooth muscle cell infiltration and collagen synthesis²⁶.

On the other hand, Treg deficiency, generated through combined genetic deficiency of *Cd80* and *Cd86*, led to a marked increase in atherosclerosis²⁷. Conversely, adoptive transfer of Tregs into *ApoE^{-/-}* mice reduced plaque burden further suggesting their atheroprotective nature²⁸. Although not always reproducible, some clinical studies have demonstrated low Treg numbers, as well as low IL-10 expression, predict cardiovascular events^{29–32}. Mechanistically, Tregs may exert their anti-atherogenic functions via interaction with antigen presenting cells (APCs), IL-2 sequestration, or expression of their own anti-inflammatory cytokines. APCs provide feedback to conventional CD4⁺ T cells through co-stimulatory molecules such as CD80/86 expressed on the APC, which interacts with T cell CD28 to stimulate the cell. However, Tregs-associated co-inhibitory molecule cytotoxic T-lymphocyte-associated protein 4 (CTLA-4) can interact with CD80/86 as well ultimately blocking conventional T cell-APC interactions³³. Furthermore, conventional T cells can be activated through autocrine and paracrine IL-2 in the local environment. However, Tregs can sequester local IL-2 through their high expression of the IL-2 receptor (CD25) depriving conventional T cells of the growth factor³⁴. Finally, Tregs can suppress the activation through expression of IL-10 and TGF-β to hamper pro-atherogenic T cell proliferation^{35,36}. However, it is important to note the anti-atherogenic effects of Tregs may diminish as the disease progresses. In late stage atherosclerosis, Tregs can present as a mixed Th1/Treg phenotype, which co-expresses FoxP3 and T-bet and loses their suppressive capacity^{37,38}.

Unlike Th1 and Tregs, the roles of Th2 and Th17 remain controversial in atherosclerosis. Th2 cells are involved in type II immune responses where they primarily express IL-4 as well as IL-13 and IL-5. After binding the IL-4 receptor (IL-4R), IL-4 activates the signaling pathway that leads to expression of signal transducer and activator of transcription 6 (STAT6)³⁹. STAT6 is a key regulator of Th2 differentiation as well as alternatively activated macrophage (M2) polarization, which is favorable for plaque regression under atherosclerotic conditions^{40,41}. Although IL-4 has been shown to oppose pro-atherogenic Th1 effects, *in vivo* studies using IL-4-deficient mice have shown an inconsistent role where it may have no effect on plaque burden^{42,43}. Importantly though, the ratio of IFN- γ to IL-4 has been shown to correlate with inflammation in other chronic inflammatory diseases such as rheumatoid arthritis, which suggests balancing traditional Th1 and Th2 responses may be of importance in atherosclerosis⁴⁴. Similar to Th2 cells, studies targeting Th17 cells have shown conflicting results. Using a double *ApoE^{-/-}Il17^{-/-}* knockout model, researchers observed a reduction in plaque in both the aortic root and arch; however, exogenous IL-17A injections also resulted in a reduction of plaque burden^{45,46}. In terms of atheroprotection, however, both mouse and human studies have indicated IL-17 may help increase collagen content and promote plaque stability^{47,48}.

In a similar vein, our understanding of the function of CD8⁺ T cells in atherosclerosis remains incomplete (Figure 1B). Genetic deficiency using a *ApoE^{-/-}CD8^{-/-}* knockout model did not result in changes to plaque size⁴⁹. However, depletion of CD8⁺ T cells using a monoclonal antibody reduced atherosclerosis and necrotic core area suggesting a pro-atherogenic role^{50,51}. CD8⁺ T cells express cytotoxic molecules such as perforin and granzyme B, which may promote apoptosis of lesional cells and therefore necrotic core formation. In addition to the reduction in atherosclerosis, CD8⁺ depleted mice expressed lower CC-motif chemokine 2 (CCL2), a chemokine involved in mobilization of monocytes towards the inflamed intima. *In vitro* co-cultures of CD8⁺ T cells with macrophages confirmed the ability of these cells to trigger CCL2 expression⁵¹. Although depletion in early stage atherosclerosis results in lower plaque burden, a second study observed opposite effects in advanced atherosclerosis. Namely, depletion of CD8⁺ T cells led to less stable lesions with increased lesional Th1 content, macrophage content, and necrotic core area⁵². Complete depletion of the CD8 component may impair regulatory CD8⁺ T cells, which appear to control pro-atherogenic germinal center B cell responses⁵³. More studies are needed to

assess the differing roles of CD8⁺ T cells considering scRNA-seq studies on human plaques report CD8⁺ cells outnumber CD4⁺ cells⁹.

Finally, little is known about NKT and $\gamma\delta$ -T cells in atherosclerosis (Figure 1C and 1D). Unlike conventional T cells with $\alpha\beta$ chains in their T cell receptors (TCRs), NKT cells have an invariant α chain while $\gamma\delta$ -T cells have a γ chain and δ chain. Both subsets act as bridges between the innate and adaptive immune system as NKT cells recognize antigen presentation through the major histocompatibility complex (MHC) class I-like protein, CD1d, while $\gamma\delta$ -T cells generally do not require antigen presentation^{54,55}. To study the effect of NKT cells in atherosclerosis, most studies use CD1d-deficient mice, which are lacking NKT cells, and have reported reductions in atherosclerosis^{56,57}. However, one study administered a prototypical CD1d ligand, alpha-Galactosylceramide (alpha-GalCer), to increase NKT activation and observed a reduction in atherosclerosis in *LDLr*^{-/-} mice⁵⁸. Following activation, NKT cells produce tremendous amounts of cytokines and can be classified in a similar manner to Th cells, namely NKT1, NKT2, NKT17 as well as others⁵⁹. Their classification corresponds to transcription factor and cytokine production as NKT1 produce T-bet and IFN- γ , NKT2 produce promyelocytic leukemia zinc finger (PLZF) and IL-4, and NKT17 produce ROR γ t and IL-17A⁶⁰. To date, no study has distinguished the contribution of individual NKT subsets to atherosclerosis, which may produce more intricate differences in atherosclerosis outcomes similar to Th cells. On the other hand, utilizing an *ApoE*^{-/-} *TCR δ* ^{-/-} model, which lacks $\gamma\delta$ -T cells, researchers observed no differences in plaque burden in early atherosclerosis⁶¹. However, $\gamma\delta$ -T cells are a known source of IL-17A, which may complicate the functions of Th17 cells⁶².

2.3. T cell activation and differentiation

Before T cells can apply their pro-atherogenic or anti-atherogenic roles, the cells need to be activated and differentiated into their unique subsets. As a general model, T cells remain in a naïve state before initial activation; however, following activation T cells expand and express lineage-specific transcription factors in order to produce cytokines that confer effector functions. After the appropriate response, effector T cell populations decline in numbers through apoptosis while the remaining effector cells convert to memory cells that are poised for rapid reactivation upon secondary stimulation⁶³.

To induce efficient initial activation, T cells initially require antigen stimulation through their TCR, which is followed by a secondary co-stimulatory signal (Figure 2)⁶⁴. A third signal, which may be in addition to the first two signals or act alone, from local pro- or anti-inflammatory cytokines can further cement the polarization⁶⁵. Ultimately, all activation signals lead to tightly regulated processes allowing for specific transcription factor and subsequent cytokine expression. However, recent studies have also observed specific epigenetic signatures in T cell subsets that allow for distinctive expression patterns suggesting an additional control in terms of T cell activation and polarization.

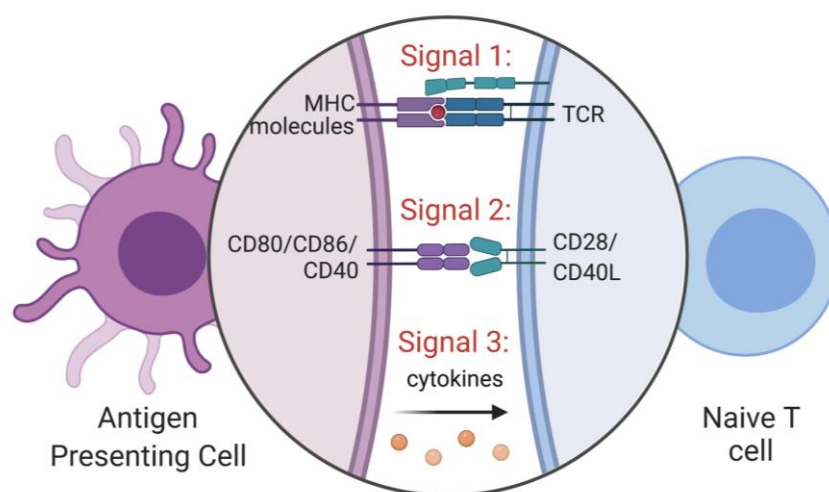


Figure 2: Signals for T cell activation. T cells are activated using three signals. First, T cells can be activated by antigen presenting cells (APCs) that present cognate ligands to T cells using their T cell receptor (TCR). Secondly, T cells require a co-stimulatory or co-inhibitory signal from APCs. These signals fall into two groups: the immunoglobulin superfamily (IgSF) and the tumor necrosis receptor superfamily (TNFRSF). The interaction between CD28 and CD80/CD86 falls under the IgSF group while the interaction between CD40L and CD40 falls under the TNFRSF group. Finally, local cytokines may also influence T cell activation. Modified from a Biorender.com template created by Anna Lazaratos.

To begin the process, antigens are first processed by APCs and later extracellular major histocompatibility complex (MHC) receptors will present smaller peptides, which will interact and form specific connections with TCRs. Subsets of T cells require different MHC classes such as CD4⁺ T cells using MHCII while CD8⁺ T cells using MHCI and, as mentioned above, NKT cells using the MHCI-like receptor CD1d⁵⁴. Although atherosclerosis-specific antigens are still under investigation, some studies have identified T cell clones which recognize epitopes from modified cholesterol molecules, like oxidized LDL (oxLDL), as well as heat shock proteins^{66,67}. More recently, autoreactive ApoB-specific T cells have been identified and phenotyped, which have been directly observed in the lymph nodes

of mice⁶⁸. Single cell analysis of ApoB-specific T cells revealed a mixed phenotype with gene expression profiles mirroring Th1, Th17, and Treg cells suggesting a potential gradient of functions^{13,68}.

Following cognate antigen recognition, co-stimulatory, as well as co-inhibitory, signaling help determine the fate of activated T cells. Although the organization of extracellular receptors is likely to be random, T cell surface markers reorganize to form an immunological synapse where co-stimulatory molecules are in close proximity to the TCR for efficient co-signaling⁶⁹. In general, co-stimulatory molecules are divided into two categories: the immunoglobulin superfamily (IgSF) and the tumor necrosis receptor superfamily (TNFRSF). Within the IgSF group, CD28 is the prototypical receptor while the CD40-CD40L dyad represents the prototypical, and most well characterized, interaction of the TNFRSF group⁶⁹. In the context of atherosclerosis, both pathways have been implicated pointing to the importance of co-stimulation in plaque development. For example, elevated numbers of circulating CD4⁺CD28^{null} T cells, meaning they lack CD28, are known to secrete high levels of IFN- γ , and have been associated with acute coronary syndrome^{70,71}. Disruption of the CD40-CD40L dyad, on the other hand, was found to greatly diminish atherosclerosis progression, but the cellular source requirements remained unknown at the time^{72,73}. The immune regulatory effects from other co-stimulatory molecules have been or still are being investigated in atherosclerosis including CD27, programmed cell death protein 1 (PD-1), CD134 (OX40), and glucocorticoid-induced tumor necrosis factor receptor (GITR)⁷⁴.

Inflammatory stimuli, such as local secretion of cytokines, can also influence the differentiation of T cells. While some CD4⁺ subsets require external cytokine signaling for effective differentiation, such as the requirement of IL-4 for Th2 cells, signal 3 cytokines appear to promote bystander effects predominately in CD8⁺ T cells^{39,65}. In particular, IL-12 as well as type I IFNs appear to be involved in accumulating efficient numbers of CD8⁺ effector cells^{75,76}. However, type II cytokines like IL-4 have also been shown to promote bystander activation of CD8⁺ T cells as well⁷⁷. External cytokine signaling, as well as co-stimulated T cells, prime activated T cells into a differentiated memory state, which allows for 'memory recall' functions where subsets can re-express effector molecules rapidly if challenged. During this process, the transcriptional landscape of the T cells and availability of lineage-specific transcription factors is likely influenced by epigenetic factors.

As mentioned in the previous section, differentiation of T cells is highly dependent on transcription factors that allow for the expression of effector cytokines and molecules;

however, recent studies have demonstrated that chromatin accessibility plays an important role in T cell differentiation and lineage-defining gene expression. Following T cell activation, upregulation of the transcription factors nuclear factor of activated T cells (NFAT) and activator protein 1 (AP-1) induced new areas of open chromatin allowing for the transcription of effector molecules⁷⁸. Within CD4⁺ Th cells, signature cytokines have been shown to hold active transcription marks, such as histone 3 lysine 4 trimethylation (H3K4me3), within their native lineage while repressive histone marks, such as H3K27me3, in all other lineages⁷⁹. While several studies have investigated the role of epigenetic reprogramming on innate immune cells and their progenitors^{80–82}, studies are lacking on the effect of lipids in reprogramming T cells and their downstream effect on atherosclerosis.

2.4. Rationale

Atherosclerosis is a global health problem characterized by chronic inflammation carried out by a diverse set of immune cells. Of these cells, T cells represent an intriguing target for novel immunotherapies in atherosclerosis as they are clearly capable of both pro-atherogenic and anti-atherogenic contributions to plaque development. Considering the importance of T cell activation in determining their fate and subsequent effect on atherosclerosis, the present work used a multi-pronged approach to target different aspects of T cell activation. First, we aimed to dissect the contribution of two separate co-stimulatory molecules, CD40L and GITR, in the chronic inflammation observed in atherosclerotic conditions. In the first study, we investigated links between sCD40L and inflammation markers, specifically IFN- γ , in human plaques. In order to find the cellular mechanism, we then employed conditional cell-specific knockout models in the two primary expressing cell types, T cells and platelets. In a second approach, we investigated a second co-stimulatory molecule, GITR, which is expressed on both Tregs and effector T cells as well as other immune cells. Previous reports on the effect of GITR have been inconclusive as both possible pro-atherogenic and anti-atherogenic have been described^{83,84}. Therefore, to extensively assess its contribution to atherogenesis, we first compared GITR expression in human symptomatic and asymptomatic carotid endarterectomies. To determine the global effect of GITR, we generated GITR-deficient mice and analyzed both immune compartments during atherogenesis as well as atherosclerotic plaque progression. Finally, we targeted the epigenetic control of T cell polarization through the H3K27me3-associated methyltransferase, Enhancer of zeste homolog 2 (EZH2). To pinpoint its contribution and cellular source, we analyzed *EZH2* expression using bulk and scRNA-seq of stable and unstable human carotid endarterectomies. To dissect the effect of EZH2 on CD4⁺ and CD8⁺ T cells, we incorporated a CD4cre as well as CD8cre model.

Altogether, the three studies provide mechanistic insights into the roles of CD40L, GITR, and EZH2 in inflammation during atherosclerosis. In particular, deficiency of CD40L and EZH2 highlight the potent effects of balancing IFN- γ and IL-4 from activated T cells during plaque progression while GITR deficiency revealed that while T cells produce large quantities of the co-stimulatory molecule monocyte expression is key player in its role in atherosclerosis.

References

1. Weber, C. & Noels, H. Atherosclerosis: current pathogenesis and therapeutic options. *Nat. Med.* **17**, 1410–1422 (2011).
2. Lozano, R. *et al.* Global and regional mortality from 235 causes of death for 20 age groups in 1990 and 2010: A systematic analysis for the Global Burden of Disease Study 2010. *Lancet* **380**, 2095–2128 (2012).
3. Lacy, M. *et al.* Interactions between dyslipidemia and the immune system and their relevance as putative therapeutic targets in atherosclerosis. *Pharmacol. Ther.* **193**, 50–62 (2019).
4. Takei, A., Huang, Y. & Lopes-Virella, M. F. Expression of adhesion molecules by human endothelial cells exposed to oxidized low density lipoprotein: Influences of degree of oxidation and location of oxidized LDL. *Atherosclerosis* **154**, 79–86 (2001).
5. Libby, P. *et al.* Atherosclerosis. *Nat. Rev. Dis. Prim.* **5**, 1–18 (2019).
6. Poels, K. *et al.* Immune Checkpoint Inhibitor Therapy Aggravates T Cell–Driven Plaque Inflammation in Atherosclerosis. *JACC CardioOncology* **2**, 599–610 (2020).
7. Robbins, C. S. *et al.* Local proliferation dominates lesional macrophage accumulation in atherosclerosis. *Nat. Med.* **19**, 1166–1172 (2013).
8. Lacy, M. *et al.* Cell-specific and divergent roles of the CD40L-CD40 axis in atherosclerotic vascular disease. *Nat. Commun.* **12**, 1–12 (2021).
9. Fernandez, D. M. *et al.* Single-cell immune landscape of human atherosclerotic plaques. *Nat. Med.* **25**, 1576–1588 (2019).
10. Depuydt, M. A. C. *et al.* Microanatomy of the Human Atherosclerotic Plaque by Single-Cell Transcriptomics. *Circ. Res.* 1437–1455 (2020) doi:10.1161/CIRCRESAHA.120.316770.
11. MacParland, S. A. *et al.* Single cell RNA sequencing of human liver reveals distinct intrahepatic macrophage populations. *Nat. Commun.* **9**, 1–21 (2018).
12. Cole, J. E. *et al.* Immune cell census in murine atherosclerosis: Cytometry by time of flight illuminates vascular myeloid cell diversity. *Cardiovasc. Res.* **114**, 1360–1371 (2018).
13. Winkels, H. & Wolf, D. Heterogeneity of T Cells in Atherosclerosis Defined by Single-Cell RNA-Sequencing and Cytometry by Time of Flight. *Arterioscler. Thromb. Vasc. Biol.* 549–563 (2021) doi:10.1161/ATVBAHA.120.312137.
14. Ridker, P. M. *et al.* Antiinflammatory Therapy with Canakinumab for Atherosclerotic Disease. *N. Engl. J. Med.* **377**, 1119–1131 (2017).
15. Libby, P. Interleukin-1 Beta as a Target for Atherosclerosis Therapy. *J. Am. Coll. Cardiol.* **70**, 2278–2289 (2017).
16. Ridker, P. M. *et al.* Low-Dose Methotrexate for the Prevention of Atherosclerotic Events. *N. Engl. J. Med.* **380**, 752–762 (2019).
17. Tardif, J.-C. *et al.* Efficacy and Safety of Low-Dose Colchicine after Myocardial Infarction. *N. Engl. J. Med.* **381**, 2497–2505 (2019).
18. Nidorf, S. M. *et al.* Colchicine in Patients with Chronic Coronary Disease. *N. Engl. J. Med.* **383**, 1838–1847 (2020).
19. Ravelli, R. B. G. *et al.* Insight into tubulin regulation from a complex with colchicine and a stathmin-like domain. *Nature* **428**, 198–202 (2004).
20. Perico, N. *et al.* Colchicine Interferes with L-Selectin and Leukocyte Function-Associated Antigen-1 Expression on Human T Lymphocytes and Inhibits T Cell Activation. *J. Am. Soc. Nephrol.* **7**, 594–601 (1996).
21. Saigusa, R., Winkels, H. & Ley, K. T cell subsets and functions in atherosclerosis. *Nat. Rev. Cardiol.* **17**, 387–401 (2020).

22. Tse, K., Tse, H., Sidney, J., Sette, A. & Ley, K. T cells in atherosclerosis. *Int. Immunol.* **25**, 615–622 (2013).
23. Buono, C. *et al.* T-bet deficiency reduces atherosclerosis and alters plaque antigen-specific immune responses. *Proc. Natl. Acad. Sci. U. S. A.* **102**, 1596–1601 (2005).
24. Whitman, S. C., Ravisankar, P. & Daugherty, A. IFN- γ deficiency exerts gender-specific effects on atherogenesis in apolipoprotein E $^{-/-}$ mice. *J. Interf. Cytokine Res.* **22**, 661–670 (2002).
25. Whitman, S. C., Ravisankar, P., Elam, H. & Daugherty, A. Exogenous interferon- γ enhances atherosclerosis in apolipoprotein E $^{-/-}$ mice. *Am. J. Pathol.* **157**, 1819–1824 (2000).
26. Amento, E. P., Ehsani, N., Palmer, H. & Libby, P. Cytokines and growth factors positively and negatively regulate interstitial collagen gene expression in human vascular smooth muscle cells. *Arterioscler. Thromb. Vasc. Biol.* **11**, 1223–1230 (1991).
27. Ait-Oufella, H. *et al.* Natural regulatory T cells control the development of atherosclerosis in mice. *Nat. Med.* **12**, 178–180 (2006).
28. Mor, A. *et al.* Role of naturally occurring CD4+CD25+ regulatory T cells in experimental atherosclerosis. *Arterioscler. Thromb. Vasc. Biol.* **27**, 893–900 (2007).
29. Mor, A., Luboshits, G., Planer, D., Keren, G. & George, J. Altered status of CD4+CD25+ regulatory T cells in patients with acute coronary syndromes. *Eur. Heart J.* **27**, 2530–2537 (2006).
30. George, J. *et al.* Regulatory T cells and IL-10 levels are reduced in patients with vulnerable coronary plaques. *Atherosclerosis* **222**, 519–523 (2012).
31. Wigren, M. *et al.* Low levels of circulating CD4+FoxP3+ T cells are associated with an increased risk for development of myocardial infarction but not for stroke. *Arterioscler. Thromb. Vasc. Biol.* **32**, 2000–2007 (2012).
32. Barth, S. D. *et al.* The Ratio of Regulatory (FOXP3+) to Total (CD3+) T Cells Determined by Epigenetic Cell Counting and Cardiovascular Disease Risk: A Prospective Case-cohort Study in Non-diabetics. *EBioMedicine* **11**, 151–156 (2016).
33. Walker, L. S. K. Treg and CTLA-4: Two intertwining pathways to immune tolerance. *J. Autoimmun.* **45**, 49–57 (2013).
34. Chinen, T. *et al.* An essential role for IL-2 receptor in regulatory T cell function. *Nat. Immunol.* **97**, 1322–1333 (2016).
35. Tiemessen, M. M. *et al.* Transforming growth factor- β inhibits human antigen-specific CD4+ T cell proliferation without modulating the cytokine response. *Int. Immunol.* **15**, 1495–1504 (2003).
36. Brooks, D. G., Walsh, K. B., Elsaesser, H. & Oldstone, M. B. A. IL-10 directly suppresses CD4 but not CD8 T cell effector and memory responses following acute viral infection. *Proc. Natl. Acad. Sci. U. S. A.* **107**, 3018–3023 (2010).
37. Butcher, M. J. *et al.* Atherosclerosis-Driven Treg Plasticity Results in Formation of a Dysfunctional Subset of Plastic IFN γ + Th1/Tregs. *Circ. Res.* **119**, 1190–1203 (2016).
38. Li, J. *et al.* CCR5+T-bet+FoxP3+ Effector CD4 T Cells Drive Atherosclerosis. *Circ. Res.* **118**, 1540–1552 (2016).
39. Walker, J. A. & McKenzie, A. N. J. TH2 cell development and function. *Nat. Rev. Immunol.* **18**, 121–133 (2018).
40. Rahman, K. *et al.* Inflammatory Ly6Chi monocytes and their conversion to M2 macrophages drive atherosclerosis regression. *J. Clin. Invest.* **127**, 2904–2915 (2017).
41. Weinstock, A. *et al.* Wnt signaling enhances macrophage responses to IL-4 and promotes resolution of atherosclerosis. *Elife* **10**, 1–28 (2021).
42. Wurtz, O., Bajénoff, M. & Guerder, S. IL-4 mediated inhibition of IFN- γ production by CD4+ T cells proceeds by several developmentally regulated mechanisms. *Int. Immunol.* **16**, 501–508 (2004).
43. King, V. L., Cassis, L. A. & Daugherty, A. Interleukin-4 does not influence development of hypercholesterolemia or angiotensin II-induced atherosclerotic lesions in mice. *Am. J. Pathol.* **171**,

- 2040–2047 (2007).
44. Scola, M. P. *et al.* Interferon- γ : Interleukin 4 ratios and associated type 1 cytokine expression in juvenile rheumatoid arthritis synovial tissue. *J. Rheumatol.* **29**, 369–378 (2002).
 45. Butcher, M. J., Gjurich, B. N., Phillips, T. & Galkina, E. V. The IL-17A/IL-17RA axis plays a proatherogenic role via the regulation of aortic myeloid cell recruitment. *Circ. Res.* **110**, 675–687 (2012).
 46. Taleb, S. *et al.* Loss of SOCS3 expression in T cells reveals a regulatory role for interleukin-17 in atherosclerosis. *J. Exp. Med.* **206**, 2067–2077 (2009).
 47. Gisterå, A. *et al.* Transforming growth factor- β signaling in T cells promotes stabilization of atherosclerotic plaques through an interleukin-17-dependent pathway. *Sci. Transl. Med.* **5**, 18–23 (2013).
 48. Brauner, S. *et al.* Augmented Th17 differentiation in Trim21 deficiency promotes a stable phenotype of atherosclerotic plaques with high collagen content. *Cardiovasc. Res.* **114**, 158–167 (2018).
 49. Elhage, R. *et al.* Deleting TCR $\alpha\beta$ + or CD4+ T lymphocytes leads to opposite effects on site-specific atherosclerosis in female apolipoprotein E-deficient mice. *Am. J. Pathol.* **165**, 2013–2018 (2004).
 50. Kyaw, T. *et al.* Cytotoxic and proinflammatory CD8+ T lymphocytes promote development of vulnerable atherosclerotic plaques in ApoE-deficient mice. *Circulation* **127**, 1028–1039 (2013).
 51. Cochain, C. *et al.* CD8+ T Cells Regulate Monopoiesis and Circulating Ly6Chigh Monocyte Levels in Atherosclerosis in Mice. *Circ. Res.* **117**, 244–253 (2015).
 52. Van Duijn, J. *et al.* CD8+ T-cells contribute to lesion stabilization in advanced atherosclerosis by limiting macrophage content and CD4+ T-cell responses. *Cardiovasc. Res.* **115**, 729–738 (2019).
 53. Clement, M. *et al.* Control of the T follicular helper-germinal center B-cell axis by CD8+ regulatory T cells limits atherosclerosis and tertiary lymphoid organ development. *Circulation* **131**, 560–570 (2015).
 54. Pellicci, D. G., Koay, H. F. & Berzins, S. P. Thymic development of unconventional T cells: how NKT cells, MAIT cells and $\gamma\delta$ T cells emerge. *Nat. Rev. Immunol.* **20**, 756–770 (2020).
 55. Nielsen, M. M., Witherden, D. A. & Havran, W. L. $\gamma\delta$ T cells in homeostasis and host defence of epithelial barrier tissues. *Nat. Rev. Immunol.* **17**, 733–745 (2017).
 56. Major, A. S. *et al.* Quantitative and qualitative differences in proatherogenic NKT cells in apolipoprotein E-deficient mice. *Arterioscler. Thromb. Vasc. Biol.* **24**, 2351–2357 (2004).
 57. Nakai, Y. *et al.* Natural killer T cells accelerate atherogenesis in mice. *Blood* **104**, 2051–2059 (2004).
 58. Van Puijvelde, G. H. M. *et al.* Effect of natural killer T cell activation on initiation of atherosclerosis. *Thromb. Haemost.* **102**, 223–230 (2009).
 59. Sag, D., Özkan, M., Kronenberg, M. & Wingender, G. Improved Detection of Cytokines Produced by Invariant NKT Cells. *Sci. Rep.* **7**, 1–9 (2017).
 60. Krovi, S. H. & Gapin, L. Invariant natural killer T cell subsets—more than just developmental intermediates. *Front. Immunol.* **9**, 1–17 (2018).
 61. Cheng, H. Y., Wu, R. & Hedrick, C. C. Gammadelta ($\gamma\delta$) T lymphocytes do not impact the development of early atherosclerosis. *Atherosclerosis* **234**, 265–269 (2014).
 62. Papotto, P. H., Ribot, J. C. & Silva-Santos, B. IL-17 + $\gamma\delta$ T cells as kick-starters of inflammation. *Nat. Immunol.* **18**, 604–611 (2017).
 63. Pennock, N. D. *et al.* T cell responses: Naïve to memory and everything in between. *Am. J. Physiol. - Adv. Physiol. Educ.* **37**, 273–283 (2013).
 64. Smith-Garvin, J. E., Koretzky, G. A. & Jordan, M. S. T Cell Activation. *Annu. Rev. Immunol.* **27**, 591–619 (2009).
 65. Kim, M. T. & Harty, J. T. Impact of inflammatory cytokines on effector and memory CD8+ T cells. *Front. Immunol.* **5**, 1–5 (2014).

-
66. Afek, A. *et al.* Immunization of low-density lipoprotein receptor deficient (LDL-RD) mice with heat shock protein 65 (HSP-65) promotes early atherosclerosis. *J. Autoimmun.* **14**, 115–121 (2000).
 67. Stemme, S. *et al.* T lymphocytes from human atherosclerotic plaques recognize oxidized low density lipoprotein. *Proc. Natl. Acad. Sci. U. S. A.* **92**, 3893–3897 (1995).
 68. Wolf, D. *et al.* Pathogenic Autoimmunity in Atherosclerosis Evolves from Initially Protective Apolipoprotein B100-Reactive CD4+T-Regulatory Cells. *Circulation* 1279–1293 (2020) doi:10.1161/CIRCULATIONAHA.119.042863.
 69. Chen, L. & Flies, D. B. Molecular mechanisms of T cell co-stimulation and co-inhibition. *Nat. Rev. Immunol.* **13**, 227–242 (2013).
 70. Dumitriu, I. E. *et al.* High levels of costimulatory receptors OX40 and 4-1BB characterize CD4+CD28 null T cells in patients with acute coronary syndrome. *Circ. Res.* **110**, 857–869 (2012).
 71. Bullenkamp, J., Dinkla, S., Kaski, J. C. & Dumitriu, I. E. Targeting T cells to treat atherosclerosis: Odyssey from bench to bedside. *Eur. Hear. J. - Cardiovasc. Pharmacother.* **2**, 194–199 (2016).
 72. Lutgens, E. *et al.* Requirement for CD154 in the progression of atherosclerosis. *Nat. Med.* **5**, 1313–1316 (1999).
 73. Schönbeck, U., Sukhova, G. K., Shimizu, K., Mach, F. & Libby, P. Inhibition of CD40 signaling limits evolution of established atherosclerosis in mice. *Proc. Natl. Acad. Sci. U. S. A.* **97**, 7458–7463 (2000).
 74. Ley, K., Gerdes, N. & Winkels, H. How co-stimulatory and co-inhibitory pathways shape atherosclerosis. *Arter. Thromb Vasc Biol* **37**, 764–777 (2017).
 75. Gately, M. K., Wolitzky, A. G., Quinn, P. M. & Chizzonite, R. Regulation of human cytolytic lymphocyte responses by interleukin-12. *Cell. Immunol.* **143**, 127–142 (1992).
 76. Xiao, Z., Casey, K. A., Jameson, S. C., Curtsinger, J. M. & Mescher, M. F. Programming for CD8 T cell memory development requires IL-12 or Type I IFN. *J. Immunol.* **182**, 2786–2794 (2009).
 77. Renkema, K. R. *et al.* IL-4 sensitivity shapes the peripheral CD8+ T cell pool and response to infection. *J. Exp. Med.* **213**, 1319–1329 (2016).
 78. Bevington, S. L. *et al.* Inducible chromatin priming is associated with the establishment of immunological memory in T cells. *EMBO J.* **35**, 515–535 (2016).
 79. Wei, G. *et al.* Global Mapping of H3K4me3 and H3K27me3 Reveals Specificity and Plasticity in Lineage Fate Determination of Differentiating CD4+ T Cells. *Immunity* **30**, 155–167 (2009).
 80. Neele, A. E. *et al.* Myeloid Kdm6b deficiency results in advanced atherosclerosis. *Atherosclerosis* **275**, 156–165 (2018).
 81. Christ, A. *et al.* Western Diet Triggers NLRP3-Dependent Innate Immune Reprogramming. *Cell* **172**, 162-175.e14 (2018).
 82. Neele, A. E. *et al.* Myeloid Ezh2 Deficiency Limits Atherosclerosis Development. *Front. Immunol.* **11**, 1–9 (2021).
 83. Meiler, S. *et al.* Constitutive GITR activation reduces atherosclerosis by promoting regulatory CD4+ T-Cell responses-brief report. *Arterioscler. Thromb. Vasc. Biol.* **36**, 1748–1752 (2016).
 84. Kim, W. J. *et al.* Glucocorticoid-induced tumour necrosis factor receptor family related protein (GITR) mediates inflammatory activation of macrophages that can destabilize atherosclerotic plaques. *Immunology* **119**, 421–429 (2006).

3. Paper I: Cell-specific and divergent roles of the CD40L-CD40 axis in atherosclerotic vascular disease

Abstract

Atherosclerosis is a major underlying cause of cardiovascular disease. Previous studies showed that inhibition of the co-stimulatory CD40 ligand (CD40L)-CD40 signaling axis profoundly attenuates atherosclerosis. As CD40L exerts multiple functions depending on the cell-cell interactions involved, we sought to investigate the function of the most relevant CD40L-expressing cell types in atherosclerosis: T cells and platelets. Atherosclerosis-prone mice with a CD40L-deficiency in CD4⁺ T cells display impaired Th1 polarization, as reflected by reduced interferon- γ production, and smaller atherosclerotic plaques containing fewer T-cells, smaller necrotic cores, an increased number of smooth muscle cells and thicker fibrous caps. Mice with a corresponding CD40-deficiency in CD11c⁺ dendritic cells phenocopy these findings, suggesting that the T cell-dendritic cell CD40L-CD40 axis is crucial in atherogenesis. Accordingly, sCD40L/sCD40 and interferon- γ concentrations in carotid plaques and plasma are positively correlated in patients with cerebrovascular disease. Platelet-specific deficiency of CD40L does not affect atherogenesis but ameliorates atherothrombosis. Our results establish divergent and cell-specific roles of CD40L-CD40 in atherosclerosis, which has implications for therapeutic strategies targeting this pathway.

Copyright Disclaimer

The following article is licensed under a Creative Commons Attribution 4.0 International License (<http://creativecommons.org/licenses/by/4.0/>), which allows reproduction without additional permission. No changes have been made to the original article. The original article was published in *Nature Communications* (doi: <https://doi.org/10.1038/s41467-021-23909-z>).

4. Paper II: Glucocorticoid-induced tumour necrosis factor receptor family-related protein (GITR) drives atherosclerosis in mice and is associated with an unstable plaque phenotype and cerebrovascular events in humans

Abstract

GITR—a co-stimulatory immune checkpoint protein—is known for both its activating and regulating effects on T-cells. As atherosclerosis bears features of chronic inflammation and autoimmunity, we investigated the relevance of GITR in cardiovascular disease (CVD). GITR expression was elevated in carotid endarterectomy specimens obtained from patients with cerebrovascular events (n=100) compared to asymptomatic patients (n=93) and correlated with parameters of plaque vulnerability, including plaque macrophage, lipid and glycophorin A content, and levels of interleukin (IL)-6, IL-12, and C-C-chemokine ligand 2. Soluble GITR levels were elevated in plasma from subjects with CVD compared to healthy controls. Plaque area in 28-week-old *Gitr*^{-/-}*Apoe*^{-/-} mice was reduced, and plaques had a favourable phenotype with less macrophages, a smaller necrotic core and a thicker fibrous cap. GITR deficiency did not affect the lymphoid population. RNA sequencing of *Gitr*^{-/-}*Apoe*^{-/-} and *Apoe*^{-/-} monocytes and macrophages revealed altered pathways of cell migration, activation, and mitochondrial function. Indeed, *Gitr*^{-/-}*Apoe*^{-/-} monocytes displayed decreased integrin levels, reduced recruitment to endothelium, and produced less reactive oxygen species. Likewise, GITR-deficient macrophages produced less cytokines and had a reduced migratory capacity. Our data reveal a novel role for the immune checkpoint GITR in driving myeloid cell recruitment and activation in atherosclerosis, thereby inducing plaque growth and vulnerability. In humans, elevated GITR expression in carotid plaques is associated with a vulnerable plaque phenotype and adverse cerebrovascular events. GITR has the potential to become a novel therapeutic target in atherosclerosis as it reduces myeloid cell recruitment to the arterial wall and impedes atherosclerosis progression.

Copyright Disclaimer

The reproduction of the following article is permitted through License #5107130039536 from Oxford University Press. No changes have been made to the original article. The original article was published in the *European Heart Journal* (doi: <https://doi.org/10.1093/eurheartj/ehaa484>).

Appendix A: Paper III: Interactions between dyslipidemia and the immune system and their relevance as putative therapeutic targets in atherosclerosis

Abstract

Cardiovascular disease (CVD) continues to be a leading cause of death worldwide with atherosclerosis being the major underlying pathology. The interplay between lipids and immune cells is believed to be a driving force in the chronic inflammation of the arterial wall during atherogenesis. Atherosclerosis is initiated as lipid particles accumulate and become trapped in vessel walls. The subsequent immune response, involving both adaptive and immune cells, progresses plaque development, which may be exacerbated under dyslipidemic conditions. Broad evidence, especially from animal models, clearly demonstrates the effect of lipids on immune cells from their development in the bone marrow to their phenotypic switching in circulation. Interestingly, recent research has also shown a long-lasting epigenetic signature from lipids on immune cells. Traditionally, cardiovascular therapies have approached atherosclerosis through lipid-lowering medications because, until recently, anti-inflammatory therapies have been largely unsuccessful in clinical trials. However, the recent Canakinumab Antiinflammatory Thrombosis Outcomes Study (CANTOS) provided pivotal support of the inflammatory hypothesis of atherosclerosis in man spurring on anti-inflammatory strategies to treat atherosclerosis. In this review, we describe the interactions between lipids and immune cells along with their specific outcomes as well as discuss their future perspective as potential cardiovascular targets.

Copyright Disclaimer

The reproduction of the following article is permitted through Elsevier, Inc., for reuse in a dissertation as an author of the article. No changes have been made to the original article. The original article was published in the *Pharmacology and Therapeutics* (doi: <https://doi.org/10.1016/j.pharmthera.2018.08.012>).

Appendix B: Paper IV: T-cell EZH2 regulates type II cytokine production: a potential therapeutic target in atherosclerosis

Abstract

Background: Immune cell infiltration by T cells, as well as other immune cells, and the associated inflammation is a well-established feature of atherosclerotic plaques. Activation and polarization are critical processes that regulate T cell function, which culminates in the production of both pro-atherogenic and anti-atherogenic populations. Therefore, targeting these pathways in T cells is an attractive way to balance the immune response. Epigenetic enzymes including the histone 3 lysine 27 methyltransferase *Enhancer of Zeste Homolog 2* (*Ezh2*) have been implicated in controlling the response and polarization of T cell subsets including helper CD4⁺ T cells, T regulatory cells, and natural killer T (NKT) cells, which prompted us to investigate its T cell-specific role in atherosclerosis.

Methods: Human carotid endarterectomy specimens were collected and analyzed for plaque stability as well as EZH2 expression. Two atherosclerotic-prone, T cell-specific *Ezh2* deficient mouse strains (*Ezh2^{fl/fl}/Cd4Cre* and *Ezh2^{fl/fl}/Cd8Cre*) were generated and fed high fat diets for 6 or 8 weeks to study atherosclerosis, respectively. Following diet administration, the immune status and atherosclerotic progression of the mice were assessed by histology, flow cytometry, and bulk and single cell RNA-sequencing (scRNA-seq).

Results: In human plaques, *Ezh2* expression was elevated in symptomatic plaques prone to rupture, and scRNA-seq indicated T cells were the primary source of EZH2 expression. T cell-specific EZH2 deficiency in *Ezh2^{fl/fl}/Cd4Cre^{tg}* mice led to a reduction in atherosclerosis with a less advanced plaque phenotype, but CD8-specific EZH2 deficiency did not affect atherogenesis. In *Ezh2^{fl/fl}/Cd4Cre^{tg}* mice, elevated expression of *Il-4* as well *Zbtb16* was identified in the descending aorta by qPCR and in CD4⁺ T cells by bulk RNA-sequencing indicating an expansion of NKT cells within the CD4⁺ compartment. Flow cytometry and scRNA-seq confirmed an increase in Plzf⁺ NKT2 cells in *Ezh2^{fl/fl}/Cd4Cre^{tg}* mice, which potentially alter disease progression. IL-4 producing CD4⁺ T cells from *Ezh2^{fl/fl}/Cd4Cre^{tg}* mice polarized macrophages *in vitro* towards *arginase1*-expressing M2 anti-inflammatory phenotype, which is likely involved in the observed reduction in atherosclerosis.

Conclusions: Our study demonstrates EZH2-deficiency expands NKT2 populations which secrete large amounts of Il-4 and allows for downstream T helper 2 and M2 polarizations contributing to the reduction in atherosclerosis.

Copyright Disclaimer

No copyright disclaimer is necessary as this is an unpublished manuscript.

**T-cell EZH2 regulates type II cytokine production: a potential therapeutic target
in atherosclerosis**

Running Title: *Lacy et al.*, “ EZH2 regulates atherosclerosis through type II cytokines”

Michael Lacy, et al.

The full author list is available on page 19

Address for correspondence:

Esther Lutgens, M.D.

Institute for Cardiovascular Prevention (IPEK)

Klinikum der Universität München, Ludwig-Maximilians-Universität München (LMU
Munich)

Pettenkofenstr. 9, D-80336 Munich, Germany

Telephone: +49 (0)89 4400 - 54672

Fax: +49 (0)89 4400 – 54352

Email: esther.lutgens@med.uni-muenchen.de

Dorothee Atzler, PhD

Institute for Cardiovascular Prevention (IPEK)

Klinikum der Universität München, Ludwig-Maximilians-Universität München (LMU
Munich)

Pettenkofenstr. 9, D-80336 Munich, Germany

Telephone: +49 (0)89 4400 - 54672

Fax: +49 (0)89 4400 – 54352

Email: dorothee.atzler@med.uni-muenchen.de

Word Count: 4129/5000

Abstract

Background: Immune cell infiltration by T cells, as well as other immune cells, and the associated inflammation is a well-established feature of atherosclerotic plaques. Activation and polarization are critical processes that regulate T cell function, which culminates in the production of both pro-atherogenic and anti-atherogenic populations. Therefore, targeting these pathways in T cells is an attractive way to balance the immune response. Epigenetic enzymes including the histone 3 lysine 27 methyltransferase Enhancer of Zeste Homolog 2 (*Ezh2*) have been implicated in controlling the response and polarization of T cell subsets including helper CD4⁺ T cells, T regulatory cells, and natural killer T (NKT) cells, which prompted us to investigate its T cell-specific role in atherosclerosis.

Methods: Human carotid endarterectomy specimens were collected and analyzed for plaque stability as well as *Ezh2* expression. Two atherosclerotic-prone, T cell-specific *Ezh2* deficient mouse strains (*Ezh2^{fl/fl}/Cd4Cre* and *Ezh2^{fl/fl}/Cd8Cre*) were generated and fed high fat diets for 6 or 8 weeks to study atherosclerosis, respectively. Following diet administration, the immune status and atherosclerotic progression of the mice were assessed by histology, flow cytometry, and bulk and single cell RNA-sequencing (scRNA-seq).

Results: In human plaques, *Ezh2* expression was elevated in symptomatic plaques prone to rupture, and scRNA-seq indicated T cells were the primary source of EZH2 expression. T cell-specific EZH2 deficiency in *Ezh2^{fl/fl}/Cd4Cre^{tg}* mice led to a reduction in atherosclerosis with a less advanced plaque phenotype, but CD8-specific EZH2 deficiency did not affect atherogenesis. In *Ezh2^{fl/fl}/Cd4Cre^{tg}* mice, elevated expression of *Il-4* as well *Zbtb16* was identified in the descending aorta by qPCR and in CD4⁺ T cells by bulk RNA-sequencing indicating an expansion of NKT cells within the CD4⁺ compartment. Flow cytometry and scRNA-seq confirmed an increase in Plzf⁺ NKT2 cells in

Ezh2^{fl/fl}/Cd4Cre^{tg} mice, which potentially alter disease progression. IL-4 producing CD4⁺ T cells from *Ezh2^{fl/fl}/Cd4Cre^{tg}* mice polarized macrophages in vitro towards arginase1-expressing M2 anti-inflammatory phenotype, which is likely involved in the observed reduction in atherosclerosis.

Conclusions: Our study demonstrates EZH2-deficiency expands NKT2 populations which secrete large amounts of IL-4 and allows for downstream T helper 2 and M2 polarizations contributing to the reduction in atherosclerosis.

Word count: 349/350

Keywords:

Atherosclerosis, T cells, methylation, epigenetics

Non-standard Abbreviations and Acronyms

C-X-C motif chemokine receptor 3	CXCR3
C-C motif chemokine receptor 6	CCR6
EZH2	Enhancer of zeste homolog 2
Foxp3	Forkhead box protein P3
H3K27me3	Histone 3 Lysine 27 trimethylation
IFN- γ	Interferon-gamma
IL-13	Interleukin-13
IL-4	Interleukin-4
NKT	Natural killer T cell
PLZF	Promyelocytic leukemia zinc finger
sc-RNAseq	Single cell RNA sequencing
Zbtb16	Zinc Finger And BTB Domain Containing 16

Clinical Perspective

What is new?

- We demonstrate the first link between *Ezh2* expression and plaque stability in humans, and we present lesional T cells as the primary source of expression using single cell RNA-sequencing
- In atherosclerotic *Ezh2^{fl/fl}/Cd4Cre^{tg}* mice, T cell-specific EZH2 deficiency protects from atherosclerosis by regulating natural killer T cell numbers and polarization
- EZH2 deficiency in T cells leads to increased type II cytokines including Il-4 and Il-13, which polarizes macrophages *in vitro* towards an alternatively activated phenotype

What are the clinical implications?

- Elevated *Ezh2* expression was associated with ruptured human plaques
- Introduction of therapies targeting T-cell EZH2 may reduce plaque inflammation and increase plaque stability

Introduction

Atherosclerosis is a chronic, lipid-driven inflammatory disorder of the vasculature, which drives a variety of the underlying pathologies of cardiovascular disease (CVD) including myocardial infarction and stroke^{1,2}. A myriad of experimental evidence, including pioneering single cell RNA-sequencing (sc-RNAseq) and mass cytometry studies, have identified several immune cell subsets as key components in human and mouse atherosclerotic lesions with T cells representing an abundance of the lesional leukocytes³⁻⁵. In particular, a human study suggests that CD4⁺ and double negative (CD4⁺CD8⁻) T cells are expanded in plaques from symptomatic patients. These T-cell subsets displayed distinct activation and differentiation patterns in symptomatic patients compared to asymptomatic patients⁶. Therefore, unraveling the specific pathways that regulate T-cell activation and differentiation in the context of atherosclerosis will detail our comprehension of atherogenesis and may have great potential to reveal novel immunotherapeutic targets.

T-cell differentiation, polarization, and activation is tightly controlled by epigenetic enzymes, which can restrict expression of lineage-specific transcription factors and cytokines in effector T cells and help maintain long-term immunological responses that may influence the outcome of chronic inflammatory diseases^{7,8}. During the course of atherosclerosis development, both CD4⁺ and CD8⁺ T cells can respond to antigen presentation or cytokine stimulation leading to polarization. CD4⁺ effector T cells, in particular, differentiate into distinct subsets leading to either pro-atherogenic T helper (Th1) cells, anti-atherogenic T regulatory (Treg) cells, or the less well understood Th2 and Th17 cells, all of which express signature cytokines including interferon (IFN)- γ , interleukin (IL)-10, IL-4, or IL-17, respectively⁹. These defined cytokines are regulated by upstream transcription factors, but more importantly the expression of fate-determining

transcription factors is dependent on epigenetic mechanisms controlling their histone methylation status¹⁰. Notably, repressive histone markers, such as trimethylation of histone 3 lysine 27 (H3K27), are pivotal in silencing ectopic Th-associated gene expression in opposing subsets¹¹.

Methylating and de-methylating enzymes carefully balance the methylation status of H3K27. The polycomb repressive complex 2 (PRC2), which relies on the SET domain of *enhancer of homolog 2 (EZH2)* for its methyltransferase activity, generates the di- and tri-methylation of the histone residue^{12–14}. In addition to its canonical histone modifying role, EZH2 has also been shown to directly methylate nonhistone substrates including the transcription factor promyelocytic leukemia zinc finger (PLZF), leading to its degradation and polarization of natural killer T (NKT) cells¹⁵, as well as stabilizing the T regulatory (Treg) signature transcription factor, forkhead box protein P3 (Foxp3)¹⁶. Conversely, removal of di- and trimethylation H3K27 residues relies on several histone demethylases including Ubiquitously transcribed tetratricopeptide repeat, X chromosome (UTX) and Jumonji domain-containing protein D3 (JMJD3), or both are also known as Lysine-specific demethylase 6A and B, respectively¹⁷. In regards to T-cell differentiation, JMJD3 appears primarily to function in CD4⁺ Th17 differentiation and CD8⁺ memory formation^{18,19}; however, EZH2 has been shown to be involved in a wide variety of T-cell subsets including the CD4⁺ T helper, Treg, NKT, and T follicular cell differentiation^{20–22}. Therefore, we focused on the methyltransferase, EZH2, and hypothesized that inhibition may influence atherosclerotic plaque development.

In the current study we found that EZH2 was highly expressed in human carotid endarterectomy specimens that exhibited features of plaque instability, and was particularly expressed by human plaque T cells. T cell-specific EZH2 deficiency in atherosclerotic *ApoE*^{-/-} mice resulted in a significant decrease in atherosclerotic plaque burden. This was mediated via propagation of a type II immune response, in particular through

NKT cells. Combining histological, flow cytometric, transcriptomic, and *in vitro* assays, we show that EZH2 deficiency regulates NKT cell expression of *Plzf* and *Il4*, ultimately polarizing macrophages and T cells to an anti-atherogenic phenotype to slow atherosclerotic progression. Taken together, T cell EZH2 may be a promising therapeutic target to reduce atherosclerotic inflammation and plaque burden while increasing plaque stability.

Methods

An expanded method section can be found in the online supplement

The data that support the findings of this study are available from the corresponding authors upon request.

Human Samples

Human carotid plaques were collected from the patients who underwent carotid endarterectomy. Plaques were identified as either stable or ruptured before subsequent gene expression analysis. First, quantitative PCR (qPCR) was employed to detect *Ezh2* expression (n=15). Following qPCR, a second cohort of stable and ruptured plaques (n=4) were then dissociated with a commercial kit “Multi Tissue Dissociation Kit 2” (Miltenyi Biotech, 130-110-203). Single-cell suspension, library preparation, and cDNA synthesis were prepared according to the instructions of 10x Genomics Chromium Platform. scRNA-seq analysis was then performed in RStudio (Version 1.3.1093) using the Seurat package (Version 4.0.2)²³. Genes were excluded if expressed in fewer than 5 cells. Cells were filtered out if fewer than 100 genes or more than 3000 genes were expressed in each cell, or the mitochondrial genes proportion was larger than 20%. SCTransform normalization²⁴ was adopted to mitigate the possible sources of variations like cell cycle as well as technique-related influence. The Uniform Manifold Approximation and Projection (UMAP) was used to convert cells into a two dimensional map.

Animal Experiments

To study the effect of EZH2 on atherosclerosis, we first generated *Ezh2^{fl/fl}* mice through insertion of loxP sites flanking exons 14 and 15 (Figure S1A)²⁵. Both exons partially code for the SET domain of EZH2, which confers methyltransferase activity. Floxed exons could be subsequently removed through cre-mediated deletion. To generate CD4⁺ and CD8⁺ cell-specific knockout mice, *Ezh2^{fl/fl}* mice were backcrossed to either *Cd4cre* (stock No: 017336, Jackson Laboratory, Bar Harbor, Maine, USA)²⁶ or *Cd8cre* mice (stock No: 008766, Jackson Laboratory, Bar Harbor, Maine, USA)²⁷. Finally, both mice strains were backcrossed at least ten times to *ApoE^{-/-}* mice (stock No. 002052, Jackson Laboratory, Bar Harbor, ME, USA) to generate atherosclerosis-prone mice.

Mice were bred and housed at the animal facility at Ludwig-Maximilians Universität München following institutional guidelines. All animal experiments were approved by the local ethical committee for animal experimentation (TVA #55.2Vet-2532.Vet_02-17-180). Early atherosclerosis was studied in *Ezh2^{fl/fl}/Cd4Cre* using a 6 week high fat diet (0.2% cholesterol, Sniff) and *Ezh2^{fl/fl}/Cd8Cre* using an 8 week high fat diet (0.2% cholesterol, Sniff). Following diet administration, mice were euthanized after intraperitoneal injection with Ketamine/Xylazine.

Results

EZH2 expression is elevated in unstable human plaques

Carotid endarterectomy was performed on human patients with carotid atherosclerosis as a stroke-preventive surgery and samples were collected as part of the Munich Vascular Biobank. Classification of plaque stability was determined through histology (Figure 1A). Quantitative PCR (qPCR) was performed on stable and unstable plaques (n=15), which revealed a 10-fold increase in EZH2 expression in unstable plaques (Figure 1B). To understand the cellular source of the elevated EZH2 expression, single cell RNA sequencing (scRNA-seq) was performed on 4 carotid endarterectomy specimens. Transcriptomic

analysis revealed endothelial cells, smooth muscle cells, myeloid cells, B cells, and T cells as the major plaque's cellular components (Figure 1C). Further characterization revealed EZH2 expression was predominantly associated with the T-cell cluster suggesting that T-cell EZH2 plays a role in the pathogenesis of atherosclerosis (Figure 1D).

Generation and baseline characteristics of T cell-specific (*Ezh2^{fl/fl}/Cd4Cre*) EZH2 deficient mice

To dissect the T cell-specific effects of EZH2 in atherosclerosis, we generated mice with a T-cell EZH2 deficiency following the double positive ($CD4^+CD8^+$) stage of thymocyte development (referred to as *Ezh2^{fl/fl}/Cd4Cre^{tg}*, Figure S1A). Mice were backcrossed to apolipoprotein E (*ApoE^{-/-}*) mice and fed a high fat diet for six weeks to induce atherosclerosis. qPCR confirmed the conditional deletion of EZH2 in $CD4^+$ T cells, specifically reduced EZH2 expression while EZH1 remained unaffected (Figure S1B in the Data Supplement). Using mass spectrometry-based analysis of histones isolated from $CD4^+$ T cells, we confirmed a decrease in H3K27 trimethylation in *Ezh2^{fl/fl}/Cd4Cre^{tg}* mice compared to their wild type littermates. Basic hematological parameters as well as lipid levels were compared between atherosclerotic knockout and control animals; however, no major differences were observed (Table S1 in the Data Supplement).

T-cell EZH2 deficiency decreases atherosclerosis

In the absence of T-cell EZH2, atherosclerotic plaque area in the aortic roots and arches of both female and male *Ezh2^{fl/fl}/Cd4Cre* mice was significantly decreased (Figure 2A and Figure S2A-B in the Data Supplement) compared to their wild type littermates, suggesting a non-sex and non-site specific effect on atherogenesis. In accordance with the reduction in atherosclerotic plaque burden, using a Virmani classification²⁸ we observed less fibrous cap atheromas (FCA) in *Ezh2^{fl/fl}/Cd4Cre^{tg}* mice compared to their wild type littermates and a larger percentage of initial xanthomas (IX), suggesting T-cell EZH2

deficiency slowed plaque progression (Figure 2B). This finding was further supported by a reduction in collagen content in *Ezh2^{fl/fl}/Cd4Cre^{tg}* mice (Figure 2C).

To first check for changes in immune cell populations, we analyzed lesional Mac3⁺ macrophage area, which remained unchanged between *Ezh2^{fl/fl}/Cd4Cre^{tg}* mice and their wildtype littermates (Figure 2D). To characterize the potential T-cell phenotype, we analyzed gene expression patterns of T cell-associated markers and cytokines in the descending aorta (Figure 2E). While *CD4* and *CD8* expression was comparable between wild type and transgenic littermates, *CD3* expression was elevated in *Ezh2^{fl/fl}/Cd4Cre^{tg}* mice. The T helper cytokines *interferon (IFN)- γ* and *interleukin (IL)-13* remained unchanged, and *IL-17A* was undetectable. Remarkably, we observed a 17-fold increase of *IL-4* transcripts in *Ezh2^{fl/fl}/Cd4Cre^{tg}* mice suggesting an underlying type II immune response.

T-cell EZH2 deficient mice have profound changes in T-cell populations

To further elucidate the underlying immune mechanisms responsible for the reduction in atherosclerotic plaque burden observed in *Ezh2^{fl/fl}/Cd4Cre^{tg}* mice, we analyzed major immune cell populations in the blood and lymphoid organs using flow cytometry. Here, we discovered that EZH2 deficiency solely affected CD3⁺ T cells, with a reduced abundance in *Ezh2^{fl/fl}/Cd4Cre^{tg}* mice, while all other immune cell types remained unchanged (Figure 3A). In-depth analysis of the T-cell compartments in the blood, lymph nodes, and spleen demonstrated that CD4⁺ T cells were predominantly affected as *Ezh2^{fl/fl}/Cd4Cre^{tg}* mice displayed decreased numbers of CD4⁺ T cells while CD8⁺ T cells were unaltered (Figure 3B). To further detail subpopulation differences in splenic CD3⁺ T cells, we used a scRNAseq approach, and were able to identify 9 clusters of T cells including several subpopulations of CD4⁺ and CD8⁺ T cells (Figure 3C) using common expression markers (Figure 3-5 in the Data Supplement). Strikingly, naive CD4⁺ and CD8⁺ T cell percentages as well as Tregs were strongly reduced in *Ezh2^{fl/fl}/Cd4Cre^{tg}* mice (Figure 3D). On the

other hand, memory CD4⁺ and CD8⁺ T cells, CD8⁺ effector T cells, and natural killer T (NKT) cells percentages were all increased in *Ezh2^{fl/fl}/Cd4Cre^{tg}* mice.

CD4⁺, but not CD8⁺, T cells contribute to the type II immune response in T-cell EZH2 deficient mice

To confirm our scRNA-seq findings, we analyzed CD4⁺ and CD8⁺ T-cell subpopulations using flow cytometry. In splenic CD4⁺ T cells, we observed a similar phenomenon to the sc-RNAseq results with a shift from naive to effector memory T cells as well as a reduction in Tregs (Figure 4A). Likewise, splenic CD8⁺ T cells displayed a prominent central memory population and a reduced naive fraction (Figure 6A in the Data Supplement). In order to unravel the effects of EZH2 on CD4⁺ versus CD8⁺ cells in atherosclerosis, we employed a second animal model, which allowed us to specifically target *EZH2* expression in CD8⁺ T cells in *ApoE^{-/-}* mice (referred to as *Ezh2^{fl/fl}/Cd8Cre^{tg}*).

qPCR verified that *EZH2* expression was indeed significantly and selectively reduced in CD8⁺ T cells and not in CD4⁺ T cells in *Ezh2^{fl/fl}/Cd8Cre^{tg}* mice (Figure 6B in the Data Supplement). No significant differences were observed in basic hematological parameters or cholesterol levels between *Ezh2^{fl/fl}/Cd8Cre^{tg}* mice and their wild-type littermates (Table S2 in the Data Supplement). Following an 8 week high fat diet, no difference between plaque burden in *Ezh2^{fl/fl}/Cd8Cre^{tg}* mice and their wild type littermates was observed (Figure 6C in the Data Supplement). We only identified slight differences in central and effector memory CD8⁺ T cells using flow cytometry (Figure 6D in the Data Supplement), but the shift was not as striking as the *Ezh2^{fl/fl}/Cd4Cre* model. Furthermore, we investigated plasma levels of type II cytokines including IL-4 and IL-13 considering the increased transcriptional abundance in the aorta of *Ezh2^{fl/fl}/Cd4Cre^{tg}* mice. However, no difference was detected between *Ezh2^{fl/fl}/Cd8Cre^{tg}* mice and their wild type littermates (Figure 6E in the Data Supplement). Together, this data suggested the CD8⁺ phenotype observed in our *Ezh2^{fl/fl}/Cd4Cre* model was not intrinsically due to EZH2 deficiency.

Likely, the activation of CD8⁺ T cells was due to a bystander effect from other IL-4 producing cells.

After excluding CD8⁺ T cells, our focus shifted to the contribution of CD4⁺ T cells to the anti-atherogenic phenotype. As mentioned previously, EZH2 deficiency led to a relative increase in CD4⁺ memory T cells, which subsequent flow cytometric data pointed to a specific increase in CD4⁺ effector memory T cells (Figure 4A). Considering the complete CD3⁺ T cell fraction was decreased in *Ezh2^{fl/fl}/Cd4Cre* mice, we observed absolute decreases in several CD4⁺ T cell subpopulations except in the effector memory compartment (Figure 4B). When comparing naive and effector T cells, this difference appeared to be caused by differences in apoptosis, as revealed by activated caspase 3/7 levels in both cell types. While EZH2-deficient naive T cells displayed higher levels of apoptosis, apoptosis in CD4⁺ effector memory T cells was unaltered, accounting for the changes in cell abundance (Figure 4C).

The profound transcriptional increase of *Il-4* expression in the aorta of our *Ezh2^{fl/fl}/Cd4Cre* mice prompted us to further investigate the origin of this apparent type II immune response in our animals. Therefore, we compared subpopulations of the effector memory cells using inflammatory chemokine markers, C-X-C motif chemokine receptor 3 (CXCR3) and C-C motif chemokine receptor 6 (CCR6), which are preferentially expressed on Th1 and Th17 cells, respectively²⁹⁻³¹. Accordingly, we observed a shift from Th1-like, CXCR3⁺CCR6⁻, cells towards Th2-like, CXCR3⁻CCR6⁻, in *Ezh2^{fl/fl}/Cd4Cre^{tg}* mice (Figure 4D). To understand if these Th2-like cells could affect vascular function systemically, we compared plasma concentrations of Th1 and Th2-associated cytokines. Here, we observed elevated concentrations of Th2-associated IL-4 and IL-13, which corroborated the increase in aortic *IL-4* transcripts of *Ezh2^{fl/fl}/Cd4Cre^{tg}* mice described above (Figure 4E). To confirm CD4⁺ T cells as cellular source of these cytokines, we stimulated CD4⁺ T cells *in vitro* for 72 hours with CD3/CD28 beads and subsequently measured

cytokine production. In the supernatant, we demonstrated *Ezh2^{fl/fl}/Cd4Cre^{tg}* CD4⁺ T cells secreted 38x more IL-4 and 6x more IL-13 than their wild type counterparts, likely implicating them in the reduction of atherosclerosis (Figure 4F).

EZH2 deficient CD4⁺ T cells polarize macrophages to an anti-inflammatory phenotype

As T-cell cytokines can have a profound effect on neighboring cells, we investigated whether *Ezh2^{fl/fl}/Cd4Cre^{tg}* T cells could polarize the other predominant lesional immune cell type, macrophages. Indeed, when bone marrow derived macrophages (BMDMs) were matured and stimulated with supernatant of stimulated T-cells from *Ezh2^{fl/fl}/Cd4Cre^{tg}*, macrophages were polarized towards an anti-inflammatory phenotype, as reflected by increased macrophage arginase 1 mRNA and protein expression (Figure 5B). Inducible nitric oxide synthase (iNOS), a key marker of inflammatory macrophages, in contrast, remained lowly expressed (Figure 5A). Although lesional macrophage percentage did not differ (Figure 2D), this data together with the increased aortic *Il-4* cytokine level suggest EZH2-deficient CD4⁺ T cells may induce an advantageous, alternatively-activated plaque macrophage phenotype, which is likely involved in the observed reduction in atherosclerosis.

Bulk CD4⁺ RNA-seq reveals NKT marker expression in EZH2-deficient T cells

To dive deeper into mechanisms driving this T-cell phenotype, we performed bulk RNA sequencing on splenic CD4⁺ T cells from *Ezh2^{fl/fl}/Cd4Cre^{tg}* mice and their wild type littermates. Using a $p_{\text{adj.}} < 0.1$, we discovered 582 differentially expressed genes. In line with the previous experiments mentioned above, we demonstrated *Ezh2^{fl/fl}/Cd4Cre^{tg}* T cells upregulated *IL-4* transcripts while shifting the balance of T helper (Th)-1 and Treg-associated cytokines, *IFN- γ* and *Foxp3*, suggesting a directed T-cell polarization (Figure 6A). Ingenuity pathway analysis reinforced these data as several IFN upstream regulators, including IFN- γ , were significantly inhibited in *Ezh2^{fl/fl}/Cd4Cre^{tg}* T cells (Figure 6B).

Further analysis of differentially expressed genes revealed upregulation of transcripts including *zinc finger and BTB domain containing 16 (Zbtb16)*, the gene coding for Promyelocytic leukemia zinc finger (Plzf), as well as *killer cell lectin-like receptor subfamily A member 1 (Klra1)* in *Ezh2^{fl/fl}/Cd4Cre^{tg}* mice (Figure 6A), which are atypical markers for effector memory cells, but are characteristic for NKT cells.

T-cell EZH2 deficient mice have increased Plzf⁺ NKT cells

To identify changes in NKT populations induced by EZH2 deficiency, we investigated NKT cell populations, which were positive for both CD3 as well as the specific NKT marker PBS-57-loaded Cd1d tetramer and can be positive for CD4. In *Ezh2^{fl/fl}/Cd4Cre^{tg}* mice, we observed a 2-fold increase of NKT cells in the spleen accompanied by an increase in PLZF protein expression (Figure 7A). Of note, NKT populations as well as PLZF expression were unchanged in the spleen of *Ezh2^{fl/fl}/Cd8Cre^{tg}* mice and their wild type littermates (Figure 7B), again ruling out CD8-specific EZH2 deficiency as the driving force in our mechanism. In-depth investigation of the *Ezh2^{fl/fl}/Cd4Cre* model showed that aortic *Zbtb16* expression was significantly upregulated in *Ezh2^{fl/fl}/Cd4Cre^{tg}* mice, suggesting Plzf-expressing NKT cells were able to infiltrate the atherosclerotic plaque (Figure 7C). As the cell abundance of these NKT cells were quite low, especially in the wild type controls, we further characterized them using our previously mentioned sc-RNAseq data where we found a 4-fold increase of NKT cells in *Ezh2^{fl/fl}/Cd4Cre^{tg}* mice. We compared gene expression between transgenic and wild type NKT cells, and we found 52 differentially expressed genes ($p_{\text{adj.}} < 0.05$). Several mitochondrial genes such as *mt-Co3* and *mt-Atp6* were differentially expressed suggesting EZH2 deficiency may affect metabolism and alter the cell's phenotype. Importantly though, *Zbtb16* expression was significantly upregulated in *Ezh2^{fl/fl}/Cd4Cre^{tg}* NKT cells corroborating our flow cytometric data and previous CD4⁺ bulk sequencing experiments. Taken together, T-cell EZH2

deficiency resulted in an accumulation of Plzf⁺ NKT2 cells, which were able to infiltrate atherosclerotic plaques and alter disease progression.

Discussion

Our study demonstrates T-cell EZH2 plays a dynamic role in T-cell differentiation, ultimately shifting the balance of pro-atherogenic and anti-atherogenic immune populations under atherosclerotic conditions. Specifically, we identified EZH2 as a T cell-specific component of human plaques, which is upregulated in unstable lesions. Deficiency of T-cell EZH2 leads to a systemic increase of the type II cytokines, IL-4 and IL-13, driving macrophage polarization and the subsequent slowing of atherosclerotic progression. Within lesions, a large variety of T cells have been described; however, their function together with the cytokines they produce are not always clear cut in the literature. Unlike the unambiguous, pro-inflammatory IFN- γ -producing Th1 cells³²⁻³⁴, T cells which produce type II cytokines remain controversial in the context of atherosclerosis. Early studies suggested contradictory evidence that IL-4 was either pro-atherogenic or not involved in the induction of atherosclerosis^{35,36}. IL-13, on the other hand, was reported to reduce atherosclerosis development and promote alternatively activated macrophage polarization³⁷. However, dissecting individual contributions of IL-4 and IL-13 is complicated by their shared receptor, IL-4 receptor (IL-4R), where signaling leads to tyrosine phosphorylation of signal transducer and activator of transcription 6 (STAT6), a transcriptional regulator of Th2 cells and macrophages that is crucial for atherosclerosis regression^{38,39}. More recently, Weinstock et al demonstrated mice deficient in both IL-4 and IL-13 were resistant to plaque regression following cholesterol reduction using ApoB-antisense oligonucleotides suggesting both cytokines are key players in macrophage-induced resolving inflammation⁴⁰.

Production of IL-4 and IL-13 is predominantly associated with Th2 cells, but innate and innate-like immune cells such as NKT, mast, and eosinophils have been implicated as

cellular sources as well. With this in mind, we initially believed the IL-4 and IL-13 was originally derived from Th2 cells in this study. However, besides a Th2 response, our data reveal a vast expansion of NKT cells in *Ezh2^{fl/fl}/Cd4Cre^{tg}* mice. NKT cells are “innate-like” CD4⁺ or double negative (CD4⁻CD8⁻) T cells, which respond quickly upon stimulation from glycolipids presented by the major histocompatibility class I (MHC-I) molecule, CD1d⁴¹. Their T cell receptor (TCR)-specificity made them attractive targets in lipid-driven diseases such as atherosclerosis; however, initial studies indicate mice deficient in NKT cells displayed lower atherosclerotic burden and inhibition of NKT activation using CD1d antagonists could attenuate established atherosclerosis^{42,43}. Upon activation, NKT cells can release T helper-associated cytokines including IFN- γ , IL-4, IL-13, and IL-17A leading to a similar classification of NKT1, NKT2, and NKT17 cells as well as others⁴⁴. To date, investigations into the individual contributions of NKT subpopulations to the development of atherosclerosis are lacking, which could differentiate pro-atherogenic and anti-atherogenic subsets in this disease.

In combination with cytokine-secretion, classification schemes of NKT development rely on three transcription factors: T-box 21 (T-bet), PLZF, and retinoic acid-related orphan receptor γ t (ROR- γ t)⁴⁵. In this study, we observed a high expression of PLZF in the expanded NKT population in *Ezh2^{fl/fl}/Cd4Cre^{tg}* mice, which is associated with NKT2 cells that predominantly secrete IL-4⁴⁵. Previously, studies have suggested two different mechanisms for EZH2-mediated PLZF regulation. In a more traditional role, EZH2 has been shown to bind multiple transcription factor genes in T helper cells including *Zbtb16*, the gene coding for PLZF protein, thereby repressing gene expression dependent on T-cell subset²⁰. In a non-canonical role, however, EZH2 has also been shown to directly methylate PLZF, which leads to its ubiquitination and degradation¹⁵. Therefore, altered gene expression or protein stability may account for differential expression in EZH2-deficient NKT cells.

Although we found the expansion of NKT2 cells, we could not distinguish NKT and peripheral type II cytokine production in the current study. Likely, both subsets contribute to the cytokine production and reduction in atherosclerosis as T cells can be polarized due to cytokines in the local environment. In a similar study, using mice lacking both EZH2 and NKT cell populations, Tumes et al demonstrated IL-4 and IL-13 production originated from NKT and not peripheral T cells²⁰. In their study, their data suggested the origin of IL-4 and IL-13 were the expanded NKT2 population, which may ultimately polarize CD4⁺ T cells towards a Th2 phenotype and induce additional type II cytokine secretion. This would need to be investigated further under atherosclerotic conditions in order for us to come to the same conclusion.

In addition to NKT cells, EZH2 deficiency affected several other T-cell populations including Tregs and CD8⁺ cells. Foxp3 acts as a transcriptional repressive mark allowing a physical interaction between itself and EZH2 to target genes for H3K27me3 repression¹⁶. Furthermore, defective induction of Foxp3 expression can be a result of overstimulation from T helper cytokines including IFN- γ or IL-4 in our case⁴⁶. In the context of atherosclerosis, Tregs have been shown to be powerful anti-inflammatory mediators⁴⁷. However, in this study, we observed a type II immune response was sufficient to resolve inflammation without the aid of Tregs. Recently, Tregs and their prototypical cytokine, IL-10, were demonstrated to halt the progression of atherosclerosis through immune dampening and polarization towards Th2 cells and M2 macrophages perhaps suggesting the IL-4/IL-13/IL-10-Th2/M2/Treg is intertwined during atherosclerotic development⁴⁸.

Additionally, CD8⁺ T cells were shifted from a naive phenotype towards a central memory phenotype in *Ezh2^{fl/fl}/Cd4Cre^{tg}* mice; however, this phenotype could not be reproduced in a CD8⁺-specific knockout model. As increased IL-4 and IL-13 plasma concentrations were absent in the CD8⁺-specific knockout model, we believe this suggests a

bystander effect due to IL-4/IL-13 activation. In a parasitic helminth model, where high type II cytokine expression is expected, this bystander effect can be observed as well⁴⁹. Ultimately, these primed CD8⁺ T cells showed enhanced control of subsequent viral infections in the parasitic model⁴⁹. Under atherosclerotic conditions, the role CD8⁺ T cells remains controversial. Mice who are deficient in CD8⁺ T cells displayed no differences in atherosclerosis⁵⁰; however, it has been suggested that CD8⁺ T cells may promote monopoiesis under hyperlipidemic conditions which may affect plaque development⁵¹. Taken together, our data suggest EZH2 is a main player in T-cell activation and differentiation by suppressing anti-atherogenic type II cytokine production suggesting it can be an interesting immunotherapeutic target. Gain of function mutations in EZH2 activity have been implicated in several lymphoid and myeloid cancers such as diffuse large B cell lymphoma and follicular lymphoma, which has spurred research into inhibitory therapeutics^{52,53}. Recently, Tazemetostat, an EZH2 inhibitor which acts as a S-adenosylmethionine-competitive inhibitor to block methyltransferase activity, received accelerated FDA approval as treatment for epithelioid sarcoma^{54,55}. Recent clinical data from the Canakinumab Anti-Inflammatory Thrombosis Outcomes Study (CANTOS) trial demonstrated immunotherapy targeting cardiovascular risk also altered cancer incidence suggesting the two diseases may be linked⁵⁶. Therefore, it's plausible to suggest a cancer therapy like EZH2 inhibition may be a promising immunotherapeutic approach for patients at high risk for atherosclerotic disease as well. In *ApoE*^{-/-} mice, intraperitoneal injection of an EZH2 inhibitor, GSK126, reduced atherosclerotic lesion following high fat diet by reducing macrophage recruitment⁵⁷. However, this study did not report on the systemic effects of EZH2 inhibition, which need to be carefully reviewed as EZH2 is a crucial regulator in a variety of cell types. Further studies are needed to clarify the powerful immunomodulatory effects of EZH2 inhibition in slowing the progression of atherosclerosis.

Authors

Michael Lacy^{1,2}, Aleksandar Janjic³, Katrin Nitz^{1,2}, Cecilia Bonfiglio¹, Mahadia Kumkum¹, Yuting Wu¹, Lucas Esteban Wange³, Donato Santovito^{1,2}, Sigrid Unterlugauer¹, Laura A Bosmans⁶, Anuroop Venkatasubramani⁴, Axel Imhof⁴, Lars Maegdefessel^{2,5,6}, Wolfgang Enard³, Christian Weber^{1,2,7}, Menno de Winther^{1,8}, Dorothee Atzler^{1,2,9*}, Esther Lutgens^{1,2,8*}.

1. Institute for Cardiovascular Prevention, Ludwig-Maximilians-University, Munich Germany
2. DZHK (German Center for Cardiovascular Research), Partner Site Munich Heart Alliance, Munich, Germany
3. Anthropology and Human Genetics, Department of Biology II, Ludwig-Maximilians-University, Planegg, Germany
4. Molecular Biology, Adolf Butenandt Institute, Ludwig-Maximilians-University, Munich Germany
5. Department for Vascular and Endovascular Surgery, Technical University Munich, Klinikum Rechts der Isar, Munich, Germany
6. Molecular Vascular Medicine Unit, Department of Medicine, Karolinska Institutet, Stockholm, Sweden
7. Munich Cluster for Systems Neurology (SyNergy), Munich, Germany
8. Department of Medical Biochemistry, Amsterdam University Medical Center, University of Amsterdam, Amsterdam, The Netherlands
9. Walter Straub Institute for Pharmacology and Toxicology, Ludwig-Maximilians-University, Munich, Germany

Acknowledgements

The authors would like to acknowledge Linda Beckers and Myrthe de Toom for their excellent histological skills. We would also like to acknowledge Yvonne Jansen for her invaluable dissection skills. Brilliant violet-conjugated tetramers of CD1d containing the α -GalCer derivative PBS57 were generously provided by the Tetramer Core Facility of the US National Institutes of Health. We thank Prof. Dr. Andreas Thiel for us gifting the CD8^{cre} mice.

Sources of Funding

This study was supported by the Deutsche Forschungsgemeinschaft [DFG 671836 to D.A., CRC 1123 to A.I, L.M., D.A., E.L., C.W. and TRR 267 to C.W.]. We also acknowledge the support from the Netherlands CardioVascular Research Initiative: the Dutch Heart Foundation, Dutch Federation of University Medical Centres, the Netherlands Organization for Health Research and Development and the Royal Netherlands Academy of Sciences for the GENIUS-II project “Generating the best evidence-based pharmaceutical targets for atherosclerosis” [CVON2017-20]. This study was also supported by the Netherlands Organization for Scientific Research (NWO) [VICI grant to E.L.]; the EU (Horizon 2020, REPROGRAM to E.L. and M.d.W.); the German Centre for Cardiovascular Research (DZHK) [TRP grant to E.L, D.A. and C.W., Shared expertise grant to M.L., D.A., Women scientist grant to D.A.] and the European Research Council [ERC consolidator grant to E.L, ERC advanced grant to C.W.]. C.W. is a Van de Laar professor of atherosclerosis.

Disclosures

These authors declare no competing interests.

References

1. Weber C, Noels H. Atherosclerosis: current pathogenesis and therapeutic options. *Nat Med* 2011;17:1410–1422. doi:10.1038/nm.2538.
2. Libby P, Buring JE, Badimon L, Hansson GK, Deanfield J, Bittencourt MS, et al. Atherosclerosis. *Nat Rev Dis Prim* 2019;5:1–18. doi:10.1038/s41572-019-0106-z.
3. Winkels H, Ehinger E, Vassallo M, Buscher K, Dinh HQ, Kobiyama K, et al. Atlas of the immune cell repertoire in mouse atherosclerosis defined by single-cell RNA-sequencing and mass cytometry. *Circ Res* 2018;122:1675–1688. doi:10.1161/CIRCRESAHA.117.312513.
4. Cole JE, Park I, Ahern DJ, Kassiteridi C, Abeam DD, Goddard ME, et al. Immune cell census in murine atherosclerosis: Cytometry by time of flight illuminates vascular myeloid cell diversity. *Cardiovasc Res* 2018;114:1360–1371. doi:10.1093/cvr/cvy109.
5. Depuydt MAC, Prange KHM, Slenders L, Örd T, Elbersen D, Boltjes A, et al. Microanatomy of the Human Atherosclerotic Plaque by Single-Cell Transcriptomics. *Circ Res* 2020:1437–1455. doi:10.1161/CIRCRESAHA.120.316770.
6. Fernandez DM, Rahman AH, Fernandez NF, Chudnovskiy A, Amir ED, Amadori L, et al. Single-cell immune landscape of human atherosclerotic plaques. *Nat Med* 2019;25:1576–1588. doi:10.1038/s41591-019-0590-4.
7. Durek P, Nordström K, Gasparoni G, Salhab A, Kressler C, de Almeida M, et al. Epigenomic Profiling of Human CD4⁺ T Cells Supports a Linear Differentiation Model and Highlights Molecular Regulators of Memory Development. *Immunity* 2016;45:1148–1161. doi:10.1016/j.immuni.2016.10.022.

-
8. Wang Z, Yin H, Lau CS, Lu Q. Histone posttranslational modifications of CD4⁺ T cell in autoimmune diseases. *Int J Mol Sci* 2016;17:1–16. doi:10.3390/ijms17101547.
 9. Saigusa R, Winkels H, Ley K. T cell subsets and functions in atherosclerosis. *Nat Rev Cardiol* 2020;17:387–401. doi:10.1038/s41569-020-0352-5.
 10. Rodriguez RM, Lopez-Larrea C, Suarez-Alvarez B. Epigenetic dynamics during CD4⁺ T cells lineage commitment. *Int J Biochem Cell Biol* 2015;67:75–85. doi:10.1016/j.biocel.2015.04.020.
 11. Wei G, Wei L, Zhu J, Zang C, Hu-Li J, Yao Z, et al. Global Mapping of H3K4me3 and H3K27me3 Reveals Specificity and Plasticity in Lineage Fate Determination of Differentiating CD4⁺ T Cells. *Immunity* 2009;30:155–167. doi:10.1016/j.immuni.2008.12.009.
 12. Schuettengruber B, Chourrout D, Vervoort M, Leblanc B, Cavalli G. Genome Regulation by Polycomb and Trithorax Proteins. *Cell* 2007;128:735–745. doi:10.1016/j.cell.2007.02.009.
 13. Müller J, Hart CM, Francis NJ, Vargas ML, Sengupta A, Wild B, et al. Histone methyltransferase activity of a Drosophila Polycomb group repressor complex. *Cell* 2002;111:197–208. doi:10.1016/S0092-8674(02)00976-5.
 14. Kuzmichev A, Nishioka K, Erdjument-Bromage H, Tempst P, Reinberg D. Histone methyltransferase activity associated with a human multiprotein complex containing the enhancer of zeste protein. *Genes Dev* 2002;16:2893–2905. doi:10.1101/gad.1035902.
 15. Vasanthakumar A, Xu D, Lun AT, Kueh AJ, Gisbergen KP, Iannarella N, et al. A non-canonical function of Ezh2 preserves immune homeostasis. *EMBO Rep* 2017;18:619–631. doi:10.15252/embr.201643237.
 16. Arvey A, Van Der Veecken J, Samstein RM, Feng Y, Stamatoyannopoulos JA,

-
- Rudensky AY. Inflammation-induced repression of chromatin bound by the transcription factor Foxp3 in regulatory T cells. *Nat Immunol* 2014;15:580–587. doi:10.1038/ni.2868.
17. Manna S, Kim JK, Baugé C, Cam M, Zhao Y, Shetty J, et al. Histone H3 Lysine 27 demethylases Jmjd3 and Utx are required for T-cell differentiation. *Nat Commun* 2015;6. doi:10.1038/ncomms9152.
 18. Liu Z, Cao W, Xu L, Chen X, Zhan Y, Yang Q, et al. The histone H3 lysine-27 demethylase Jmjd3 plays a critical role in specific regulation of Th17 cell differentiation. *J Mol Cell Biol* 2015;7:505–516. doi:10.1093/jmcb/mjv022.
 19. Yamada T, Nabe S, Toriyama K, Suzuki J, Inoue K, Imai Y, et al. Histone H3K27 Demethylase Negatively Controls the Memory Formation of Antigen-Stimulated CD8 + T Cells . *J Immunol* 2019;202:1088–1098. doi:10.4049/jimmunol.1801083.
 20. Tumes D, Hirahara K, Papadopoulos M, Shinoda K, Onodera A, Kumagai J, et al. Ezh2 controls development of natural killer T cells, which cause spontaneous asthma-like pathology. *J Allergy Clin Immunol* 2019;144:549-560.e10. doi:10.1016/j.jaci.2019.02.024.
 21. Tumes DJ, Onodera A, Suzuki A, Shinoda K, Endo Y, Iwamura C, et al. The Polycomb protein Ezh2 regulates differentiation and plasticity of CD4+ T helper Type 1 and type 2 cells. *Immunity* 2013;39:819–832. doi:10.1016/j.immuni.2013.09.012.
 22. Li F, Zeng Z, Xing S, Gullicksrud JA, Shan Q, Choi J, et al. Ezh2 programs T FH differentiation by integrating phosphorylation-dependent activation of Bcl6 and polycomb-dependent repression of p19Arf. *Nat Commun* 2018;9. doi:10.1038/s41467-018-07853-z.
 23. Butler A, Hoffman P, Smibert P, Papalexi E, Satija R. Integrating single-cell

-
- transcriptomic data across different conditions, technologies, and species. *Nat Biotechnol* 2018;36:411–420. doi:10.1038/nbt.4096.
24. Hafemeister C, Satija R. Normalization and variance stabilization of single-cell RNA-seq data using regularized negative binomial regression. *Genome Biol* 2019;20:1–15. doi:10.1186/s13059-019-1874-1.
 25. Shen X, Liu Y, Hsu YJ, Fujiwara Y, Kim J, Mao X, et al. EZH1 Mediates Methylation on Histone H3 Lysine 27 and Complements EZH2 in Maintaining Stem Cell Identity and Executing Pluripotency. *Mol Cell* 2008;32:491–502. doi:10.1016/j.molcel.2008.10.016.
 26. Sawada S, Scarborough JD, Killeen N, Littman DR. A lineage-specific transcriptional silencer regulates CD4 gene expression during T lymphocyte development. *Cell* 1994;77:917–929. doi:10.1016/0092-8674(94)90140-6.
 27. Maekawa Y, Minato Y, Ishifune C, Kurihara T, Kitamura A, Kojima H, et al. Notch2 integrates signaling by the transcription factors RBP-J and CREB1 to promote T cell cytotoxicity. *Nat Immunol* 2008;9:1140–1147. doi:10.1038/ni.1649.
 28. Virmani R, Kolodgie FD, Burke AP, Farb A, Schwartz SM. Lessons From Sudden Coronary Death. *Arterioscler Thromb Vasc Biol* 2000;20:1262–1275. doi:10.1161/01.atv.20.5.1262.
 29. Yu X, Wang M, Cao Z. Reduced CD4+T Cell CXCR3 Expression in Patients With Allergic Rhinitis. *Front Immunol* 2020;11:1–9. doi:10.3389/fimmu.2020.581180.
 30. Acosta-Rodriguez E V., Rivino L, Geginat J, Jarrossay D, Gattorno M, Lanzavecchia A, et al. Surface phenotype and antigenic specificity of human interleukin 17-producing T helper memory cells. *Nat Immunol* 2007;8:639–646. doi:10.1038/ni1467.

-
31. Coursey TG, Gandhi NB, Volpe EA, Pflugfelder SC, De Paiva CS. Chemokine receptors CCR6 and CXCR3 are necessary for CD4⁺ T cell mediated ocular surface disease in experimental dry eye disease. *PLoS One* 2013;8. doi:10.1371/journal.pone.0078508.
 32. Buono C, Binder CJ, Stavrakis G, Witztum JL, Glimcher LH, Lichtman AH. T-bet deficiency reduces atherosclerosis and alters plaque antigen-specific immune responses. *Proc Natl Acad Sci U S A* 2005;102:1596–1601. doi:10.1073/pnas.0409015102.
 33. Buono C, Come CE, Stavrakis G, Maguire GF, Connelly PW, Lichtman AH. Influence of interferon- γ on the extent and phenotype of diet-induced atherosclerosis in the LDLR-deficient mouse. *Arterioscler Thromb Vasc Biol* 2003;23:454–460. doi:10.1161/01.ATV.0000059419.11002.6E.
 34. Gupta S, Pablo AM, Jiang XC, Wang N, Tall AR, Schindler C. IFN- γ , potentiates atherosclerosis in ApoE knock-out mice. *J Clin Invest* 1997;99:2752–2761. doi:10.1172/JCI119465.
 35. King VL, Cassis LA, Daugherty A. Interleukin-4 does not influence development of hypercholesterolemia or angiotensin II-induced atherosclerotic lesions in mice. *Am J Pathol* 2007;171:2040–2047. doi:10.2353/ajpath.2007.060857.
 36. King VL, Szilvassy SJ, Daugherty A. Interleukin-4 deficiency decreases atherosclerotic lesion formation in a site-specific manner in female LDL receptor^{-/-} mice. *Arterioscler Thromb Vasc Biol* 2002;22:456–461. doi:10.1161/hq0302.104905.
 37. Cardilo-Reis L, Gruber S, Schreier SM, Drechsler M, Papac-Milicevic N, Weber C, et al. Interleukin-13 protects from atherosclerosis and modulates plaque composition by skewing the macrophage phenotype. *EMBO Mol Med* 2012;4:1072–1086. doi:10.1002/emmm.201201374.

-
38. Junttila IS. Tuning the cytokine responses: An update on interleukin (IL)-4 and IL-13 receptor complexes. *Front Immunol* 2018;9.
doi:10.3389/fimmu.2018.00888.
 39. Rahman K, Vengrenyuk Y, Ramsey SA, Vila NR, Girgis NM, Liu J, et al. Inflammatory Ly6Chi monocytes and their conversion to M2 macrophages drive atherosclerosis regression. *J Clin Invest* 2017;127:2904–2915.
doi:10.1172/JCI75005.
 40. Weinstock A, Rahman K, Yaacov O, Nishi H, Menon P, Nikain CA, et al. Wnt signaling enhances macrophage responses to IL-4 and promotes resolution of atherosclerosis. *Elife* 2021;10:1–28. doi:10.7554/eLife.67932.
 41. Krovi SH, Gapin L. Invariant natural killer T cell subsets-more than just developmental intermediates. *Front Immunol* 2018;9:1–17.
doi:10.3389/fimmu.2018.01393.
 42. Nakai Y, Iwabuchi K, Fujii S, Ishimori N, Dashtsoodol N, Watano K, et al. Natural killer T cells accelerate atherogenesis in mice. *Blood* 2004;104:2051–2059.
doi:10.1182/blood-2003-10-3485.
 43. Li Y, Kanellakis P, Hosseini H, Cao A, Deswaerte V, Tipping P, et al. A CD1d-dependent lipid antagonist to NKT cells ameliorates atherosclerosis in ApoE^{-/-} mice by reducing lesion necrosis and inflammation. *Cardiovasc Res* 2016;109:305–317. doi:10.1093/cvr/cvv259.
 44. Godfrey DI, Uldrich AP, Mccluskey J, Rossjohn J, Moody DB. The burgeoning family of unconventional T cells. *Nat Immunol* 2015;16:1114–1123.
doi:10.1038/ni.3298.
 45. Klibi J, Amable L, Benlagha K. A focus on natural killer T-cell subset characterization and developmental stages. *Immunol Cell Biol* 2020;98:358–368.
doi:10.1111/imcb.12322.

-
46. Yang XP, Jiang K, Hirahara K, Vahedi G, Afzali B, Sciume G, et al. EZH2 is crucial for both differentiation of regulatory T cells and T effector cell expansion. *Sci Rep* 2015;5:1–14. doi:10.1038/srep10643.
 47. Ait-Oufella H, Salomon BL, Potteaux S, Robertson A-KL, Gourdy P, Zoll J, et al. Natural regulatory T cells control the development of atherosclerosis in mice. *Nat Med* 2006;12:178–180. doi:10.1038/nm1343.
 48. Sharma M, Schlegel MP, Afonso MS, Brown EJ, Rahman K, Weinstock A, et al. Regulatory T cells license macrophage pro-resolving functions during atherosclerosis regression. *Circ Res* 2020;127:335–353. doi:10.1161/CIRCRESAHA.119.316461.
 49. Rolot M, Dougall AM, Chetty A, Javaux J, Chen T, Xiao X, et al. Helminth-induced IL-4 expands bystander memory CD8⁺ T cells for early control of viral infection. *Nat Commun* 2018;9. doi:10.1038/s41467-018-06978-5.
 50. Elhage R, Gourdy P, Brauchet L, Jawien J, Fouque MJ, Fiévet C, et al. Deleting TCR $\alpha\beta$ ⁺ or CD4⁺ T lymphocytes leads to opposite effects on site-specific atherosclerosis in female apolipoprotein E-deficient mice. *Am J Pathol* 2004;165:2013–2018. doi:10.1016/S0002-9440(10)63252-X.
 51. Cochain C, Koch M, Chaudhari SM, Busch M, Pelisek J, Boon L, et al. CD8⁺ T Cells Regulate Monopoiesis and Circulating Ly6Chigh Monocyte Levels in Atherosclerosis in Mice. *Circ Res* 2015;117:244–253. doi:10.1161/CIRCRESAHA.117.304611.
 52. Béguelin W, Teater M, Meydan C, Hoehn KB, Phillip JM, Soshnev AA, et al. Mutant EZH2 Induces a Pre-malignant Lymphoma Niche by Reprogramming the Immune Response. *Cancer Cell* 2020;37:655-673.e11. doi:10.1016/j.ccell.2020.04.004.
 53. Lund K, Adams PD, Copland M. EZH2 in normal and malignant hematopoiesis.

-
- Leukemia 2014;28:44–49. doi:10.1038/leu.2013.288.
54. Duan R, Du W, Guo W. EZH2: A novel target for cancer treatment. *J Hematol Oncol* 2020;13:1–12. doi:10.1186/s13045-020-00937-8.
55. Kang N, Eccleston M, Clermont PL, Latarani M, Male DK, Wang Y, et al. EZH2 inhibition: A promising strategy to prevent cancer immune editing. *Epigenomics* 2020;12:1457–1476. doi:10.2217/epi-2020-0186.
56. Ridker PM, Everett BM, Thuren T, MacFadyen JG, Chang WH, Ballantyne C, et al. Antiinflammatory Therapy with Canakinumab for Atherosclerotic Disease. *N Engl J Med* 2017;377:1119–1131. doi:10.1056/nejmoa1707914.
57. Wei X, Zhang Y, Xie L, Wang K, Wang X. Pharmacological inhibition of EZH2 by GSK126 decreases atherosclerosis by modulating foam cell formation and monocyte adhesion in apolipoprotein E-deficient mice. *Exp Ther Med* 2021;22. doi:10.3892/etm.2021.10273.
58. Renaud G, Stenzel U, Maricic T, Wiebe V, Kelso J. DeML: Robust demultiplexing of Illumina sequences using a likelihood-based approach. *Bioinformatics* 2015;31:770–772. doi:10.1093/bioinformatics/btu719.
59. Parekh S, Ziegenhain C, Vieth B, Enard W, Hellmann I. zUMIs - A fast and flexible pipeline to process RNA sequencing data with UMIs. *Gigascience* 2018;7:1–9. doi:10.1093/gigascience/giy059.
60. Dobin A, Davis CA, Schlesinger F, Drenkow J, Zaleski C, Jha S, et al. STAR: Ultrafast universal RNA-seq aligner. *Bioinformatics* 2013;29:15–21. doi:10.1093/bioinformatics/bts635.
61. Fleming SJ, Marioni JC, Babadi M. CellBender remove-background: A deep generative model for unsupervised removal of background noise from scRNA-seq datasets. *BioRxiv* 2019. doi:10.1101/791699.

62. Love MI, Huber W, Anders S. Moderated estimation of fold change and dispersion for RNA-seq data with DESeq2. *Genome Biol* 2014;15:1–21. doi:10.1186/s13059-014-0550-8.
63. Krämer A, Green J, Pollard J, Tugendreich S. Causal analysis approaches in ingenuity pathway analysis. *Bioinformatics* 2014;30:523–530. doi:10.1093/bioinformatics/btt703.

Figures and Figure Legends

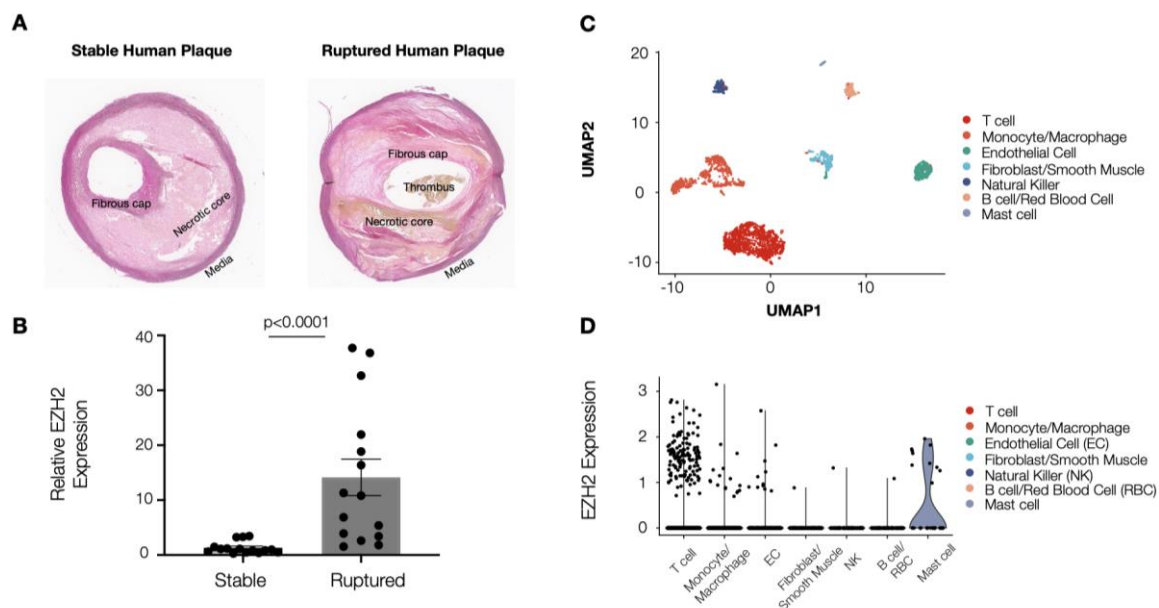


Figure 1 *EZH2* expression is associated with T cells in unstable human plaques

A, Representative histological images of stable and ruptured human plaques with labelled plaque components from patients undergoing carotid endarterectomies. **B**, Gene expression analysis using qPCR to evaluate *Ezh2* expression in stable and ruptured carotid endarterectomy specimens (n=15). Data are represented as mean \pm s.e.m. and analyzed using a two-tailed Mann-Whitney test. **C**, Single cell transcriptomes of cells isolated from carotid endarterectomy specimens were analyzed using the Uniform Manifold Approximation and Projection (UMAP) to convert cells into a two dimensional map and identify individual cell clusters (n=4). **D**, Normalized *Ezh2* gene expression per cell is displayed for individual cell clusters.

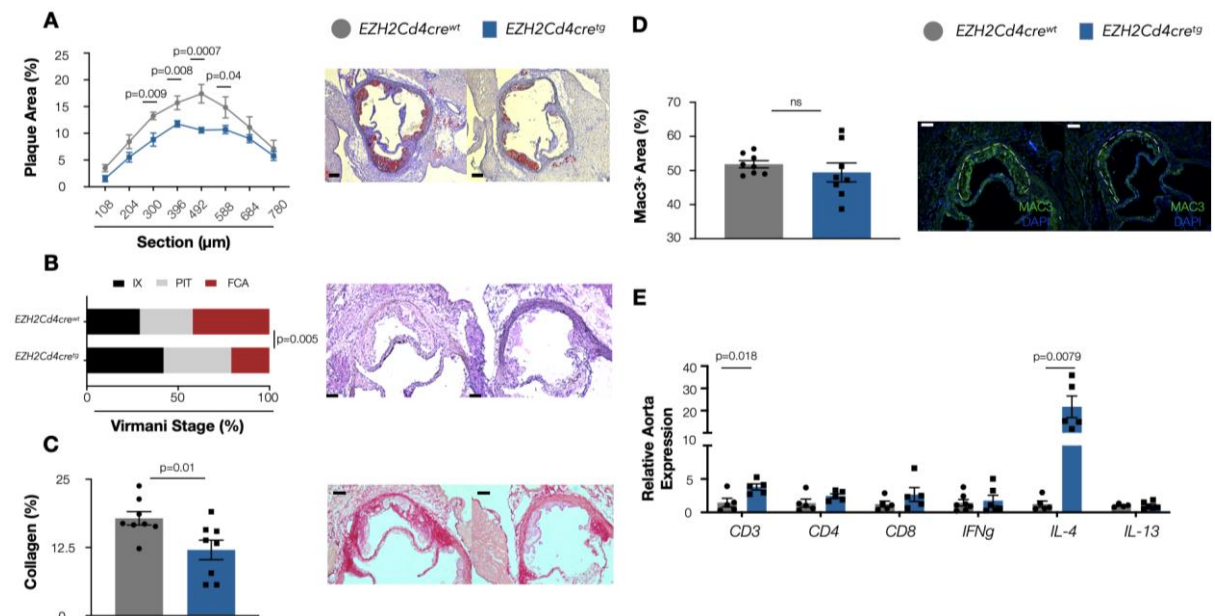


Figure 2 T-cell specific EZH2 deficiency reduces plaque burden with elevated aortic *Il-4* expression

A, Atherosclerotic plaque area across the aortic root in female *Ezh2^{fl/fl}/Cd4Cre* mice (n=8-10) at the indicated positions (left) with representative Oil Red O-stained images (right, scale bar: 200 μ m). **B**, Morphological plaque phenotype comparison (right) using a Virmani classification describing initial xanthoma (IX), pathological intima thickening (PIT), and fibrous cap atheroma phenotypes and analyzed using a Chi-square distribution analysis (n= 8 animals/24 lesions) together with representative hematoxylin and eosin stained images (right, scale bar: 100 μ m). **C-D**, Histological and immunofluorescent quantification assessing measures of plaque stability including **(C)** collagen content through Sirius red analysis and **(D)** macrophage ($Mac3^+$) content (n=8, scale bar: 100 μ m). **E**, Gene expression of T-cell associated transcripts in the descending aorta using qPCR (n=4-7). Data are all represented as mean \pm s.e.m. and analyzed using either a two-tailed Student's *t* test (**A**, **C**, **D**) or two-tailed Mann-Whitney test (**E**). CD cluster of differentiation. IFN- γ interferon-gamma. IL-4 interleukin-4. IL-13 interleukin-13.

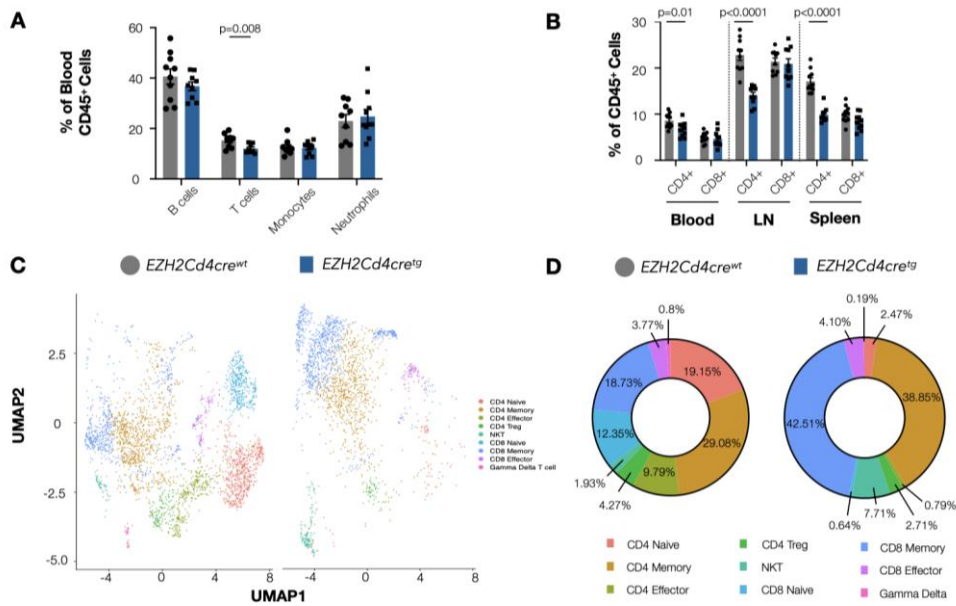


Figure 3 T-cell specific EZH2 deficiency disrupts T cell populations with major shifts in naïve, effector, and NKT compartments

A, Flow cytometric analysis of major blood cell populations in female *Ezh2^{fl/fl}/Cd4Cre* mice (n=9-10). **B**, Further flow cytometric analysis of the CD4⁺ and CD8⁺ compartments in the blood, lymph nodes (LN), and spleen (n=10). Data for (**A-B**) are represented as mean \pm s.e.m. and analyzed using a two-tailed Student's *t* test. **C**, Single cell transcriptomes of splenic CD3⁺ cells isolated from female *Ezh2^{fl/fl}/Cd4Cre* mice were analyzed using the Uniform Manifold Approximation and Projection (UMAP) to convert cells into a two dimensional map and identify individual cell clusters (n=4). **D**, Doughnut chart visualizing the proportion of each T cell cluster identified using their single cell transcriptome. CD cluster of differentiation, NKT natural killer T cell.

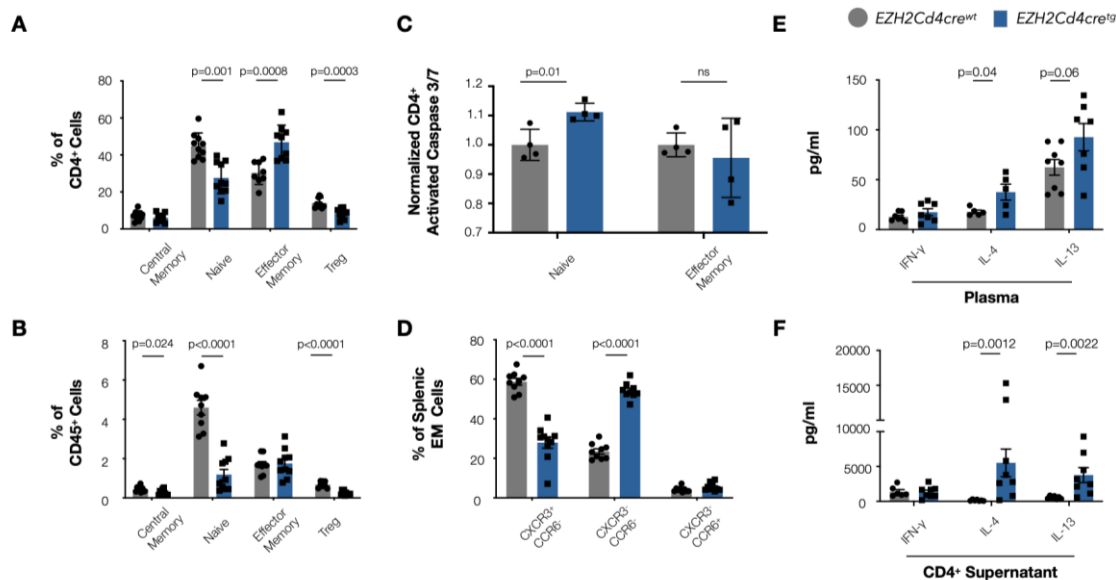


Figure 4 Flow cytometry confirms shift towards IL-4 producing, Th2-like effector

CD4⁺ T cells in *Ezh2^{fl/fl}/Cd4Cre^{tg}* mice

A-B, Flow cytometric analysis of splenic CD4⁺ populations including central memory, naïve, effector memory, and Treg (T regulatory) cells relative to all (**A**) CD4⁺ cells or to all (**B**) CD45⁺ leukocytes (n=9-10). **C**, Normalized protein expression of the apoptosis marker, activated caspase 3/7, analyzed by flow cytometry in CD4⁺ naïve and effector memory cells (n=4). **D**, Further flow cytometric analysis of the effector memory (EM) compartment in the spleen comparing CXCR3⁺CCR6⁻ (Th1-like), CXCR3⁻CCR6⁻ (Th2-like), and CXCR3⁻CCR6⁺ (Th17-like) cells (n=9-10). **E-F**, Multiplexed type I and type II cytokine measurements from the (**E**) plasma (n=5-8) or (**F**) *in vitro* cultured CD4⁺ supernatant (n=7-8) from *Ezh2^{fl/fl}/Cd4Cre* mice. Data are represented as mean ± s.e.m. and analyzed using either a two-tailed Student's *t* test (**A, B**: central memory, naïve, Treg, **C, D**: CXCR3⁺CCR6⁻, CXCR3⁻CCR6⁺, **E**) or two-tailed Mann-Whitney test (**B**: effector memory, **D**: CXCR3⁻CCR6⁻, **F**). IFN-γ interferon-gamma. IL-4 interleukin-4. IL-13 interleukin-13.

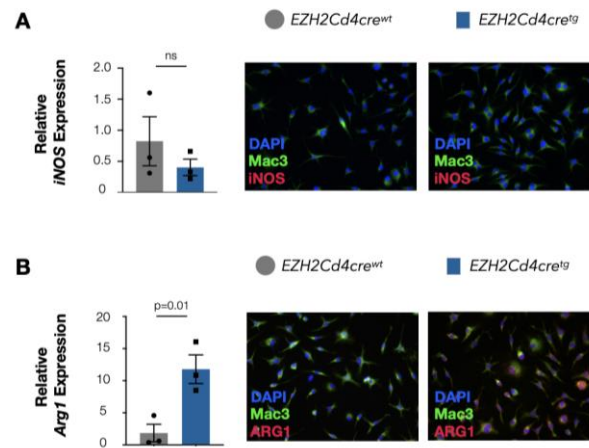


Figure 5 IL-4 producing CD4⁺ T cells in *Ezh2^{fl/fl}/Cd4Cre^{tg}* mice polarize macrophages to an alternatively activated phenotype

In vitro polarization of bone marrow derived macrophages using CD4⁺ supernatant from either from *Ezh2^{fl/fl}/Cd4Cre^{tg}* mice or their wild-type littermates. **A**, Gene expression (left) analysis using qPCR and protein expression (right) using immunofluorescence to compare expression of inducible nitric oxide synthase (iNOS) as a marker for M1 polarization (n=3). **B**, Gene expression (left) analysis using qPCR and protein expression (right) using immunofluorescence to compare expression of Arginase1 (Arg1) as a marker for M2 polarization (n=3). Data are all represented as mean \pm s.e.m. and analyzed using a two-tailed Student's *t* test

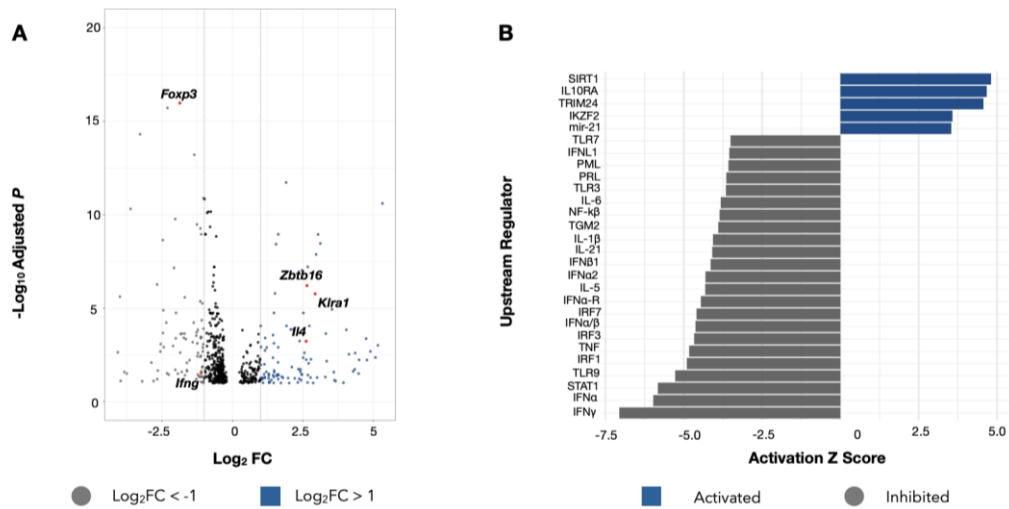


Figure 6 Bulk transcriptomic analysis confirms *Il-4* expression and identifies the NKT2-associated gene, *Zbtb16*, in CD4^+ T cells from *Ezh2^{fl/fl}/Cd4Cre^{tg}* mice

A, Volcano plot of differentially expressed genes between CD4^+ T cells isolated from the spleens of *Ezh2^{fl/fl}/Cd4Cre^{tg}* mice or their wild-type littermates (n=4-5). Data was analyzed using DeSEQ2 with significance noted as a $p_{\text{adj.}} < 0.1$ (corrected Benjamini-Hochberg). **B**, Ingenuity pathway analysis using the bulk transcriptomic data to identify inhibited (grey) and activated (blue) pathways in *Ezh2^{fl/fl}/Cd4Cre^{tg}* CD4^+ T cells.

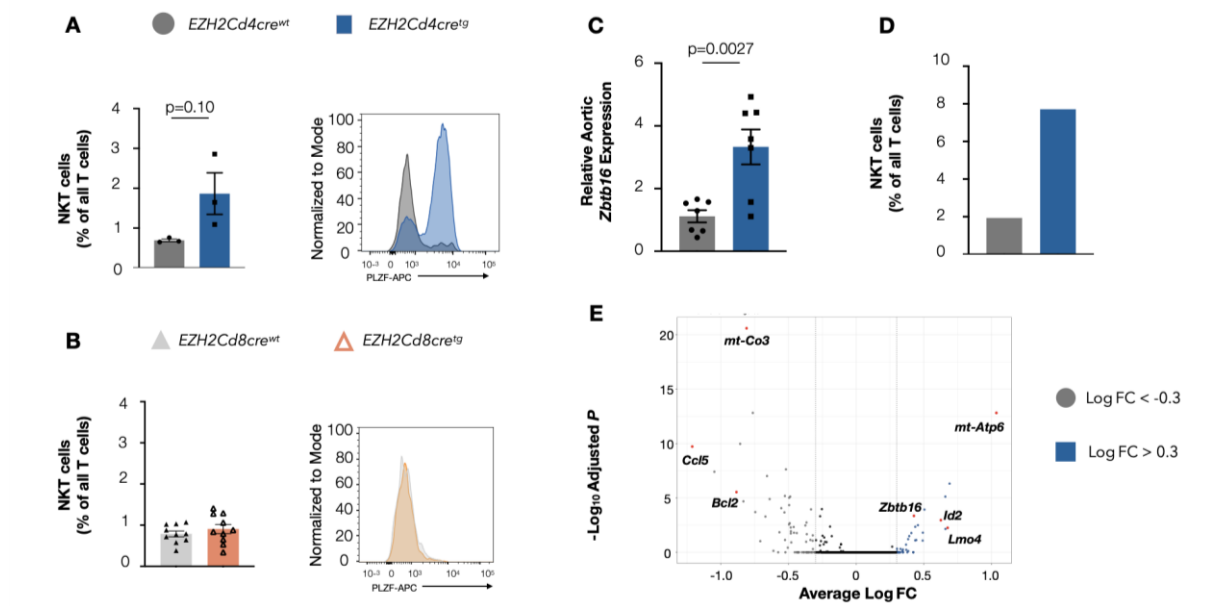


Figure 7 T-cell specific EZH2 deficiency results in increased frequency of Plzf⁺ NKT2 cells

A-B, Flow cytometric analysis (left) of splenic natural killer T (NKT) cells from **(A)** *Ezh2^{fl/fl}/Cd4Cre^{tg}* mice (n=3) and **(B)** *Ezh2^{fl/fl}/Cd8Cre^{tg}* mice (n=9-10) and their respective wild type littermates. Histogram (right) displaying comparison of promyelocytic leukemia zinc finger (Plzf) protein expression in NKT cells from both mouse strains. **C**, Gene expression of *Zbtb16* in the descending aorta using qPCR in *Ezh2^{fl/fl}/Cd4Cre* mice (n=7). **D**, Bar plot of NKT percentages identified in scRNA-seq analysis using splenic CD3⁺ from *Ezh2^{fl/fl}/Cd4Cre* mice (n=4). **E**, Differential gene expression analysis of NKT cluster using normalized counts from scRNA-seq analysis.

T-cell EZH2 regulates type II cytokine production: a potential therapeutic target in atherosclerosis

Lacy: EZH2 regulates atherosclerosis through type II cytokines

Michael Lacy, et al.

Correspondence:

Esther Lutgens, M.D.

Institute for Cardiovascular Prevention (IPEK)

Klinikum der Universität München, Ludwig-Maximilians-Universität München (LMU Munich)

Pettenkoferstr. 9, D-80336 Munich, Germany

Telephone: +49 (0)89 4400 - 54672

Fax: +49 (0)89 4400 – 54352

Email: esther.lutgens@med.uni-muenchen.de

Dorothee Atzler, PhD

Institute for Cardiovascular Prevention (IPEK)

Klinikum der Universität München, Ludwig-Maximilians-Universität München (LMU Munich)

Pettenkoferstr. 9, D-80336 Munich, Germany

Telephone: +49 (0)89 4400 - 54672

Fax: +49 (0)89 4400 – 54352

Email: dorothee.atzler@med.uni-muenchen.de

- SUPPLEMENTAL MATERIAL -

Expanded Materials and Methods

Mass spectrometry

T cells treated with C13-glucose (with or without ATPCL inhibitor) were washed once with PBS and snap-frozen in liquid nitrogen. For histone post-translational modification analysis, acid extraction with approximately 1 million cells was performed. Pelleted cells were resuspended in 100 μ L of 0.2M H₂SO₄ and histones were extracted by rotating overnight at 4°C. Cell debris were removed by centrifugation at 20,817 g (max. Speed) for 10 min at 4°C. Histone were precipitated by adding trichloroacetic acid (ThermoScientific, Cat. No 85183) to reach 26% final concentration. Tubes were mixed and incubated at 4°C for 2 hr and spun at 20,817 g for 15 min. Pellets were washed thrice with ice-cold 100% acetone (VWR, Cat. No AA22928-K2) (5 min rotation at 4°C, 15 min of 20,817 g spin at 4°C between washes), dried for 15 min at room temperature and resuspended in 20 μ L of 1x Laemmli sample buffer per million cells and boiled at 95°C for 5 min. Samples were stored at -20°C until further use. The histones corresponding to 0.5 million cells were separated using 4–20% pre-cast polyacrylamide gels (Serva, Cat. No 43277.01). Gels were briefly stained with InstantBlue Coomassie Protein Stain (abcam, Cat. No ab119211). For targeted mass-spectrometry analysis, histones bands were excised, washed once with MS-grade water (Sigma Aldrich, Cat. No 1153331000) and de-stained twice (or until transparent) by incubating 30 min at 37°C with 200 μ L of 50% acetonitrile (ACN) (CARL ROTH, Cat. No 8825.2) in 50 mM NH₄HCO₃ (CARL ROTH, Cat. No T871.1). Gel pieces were then washed twice with 200 μ L MS-grade and twice with 200 μ L of 100% ACN to dehydrate them. Histones were in-gel acylated by adding 20 μ L of propionic anhydride (Sigma-Aldrich, Cat. No 175641) and 40 μ L of 100 mM NH₄HCO₃. After 5 min, 140 μ L of 1 M NH₄HCO₃ was slowly added to the reaction. pH was checked for each sample to be around 7 (In cases

where pH was acidic, a few microlitres of 1M NH_4HCO_3 was added). Samples were incubated at 37°C for 45 min at 550 rpm. Following this, samples were washed 5 times with 200 μL of 100 mM NH_4HCO_3 , 4 times with 200 μL of MS-grade water and 4 times with 200 μL of 100% ACN. They were spun down briefly and all remaining ACN was removed. Gel pieces were rehydrated in 50 μL of trypsin solution (25 ng/ mL trypsin in 100 mM NH_4HCO_3) (Promega, Cat. No V5111) with 1 μL spike tides and incubated at 4°C for 20 min. After the addition of 150 μL of 50 mM NH_4HCO_3 , histones were in-gel digested overnight at 37°C at 550 rpm. Peptides were sequentially extracted by incubating 10 min at room temperature with 150 μL of 50 mM NH_4HCO_3 , twice with 150 μL of 50% ACN (in MS-grade water) 0.1% trifluoroacetic acid (TFA) and twice 100 μL of 100% ACN. During each of the washing steps, samples were sonicated for 3 min in a water bath followed by a brief spin down. Obtained peptides were dried using a centrifugal evaporator and stored at -20°C until resuspension in 30 μL of 0.1% TFA. For desalting, peptides were loaded in a C18 StageTip (prewashed with 20 μL of methanol followed by 20 μL 80% ACN 0.1% TFA and equilibrated with 20 μL of 0.1% TFA), washed 2 times with 20 μL of 0.1% TFA and peptides were eluted 3 times with 10 μL of 80% ACN 0.25% TFA. Flow through obtained from loading of peptides in C18, were further desalted with TopTip Carbon (glygen, Cat, No TT1CAR.96) by loading the flow through thrice (prewashed thrice with 30 μL of 100% ACN followed by equilibration thrice with 30 μL of 0.1% TFA), washed 5 times with 30 μL of 0.1% TFA and eluted thrice with 15 μL of 70% ACN and 0.1% TFA. Eluted peptides from both desalting steps were combined and evaporated in a centrifugal evaporator, resuspended in 17 μL of 0.1% TFA and stored at -20°C. Resuspended samples were injected in an Ultimate 3000 RSLCnano system (Thermo) separated in a 25-cm Aurora column (Ion-opticks) with a 50-min gradient from 6 to 43% of 80% acetonitrile in 0.1% formic acid with a 50-min gradient from 5 to 60% acetonitrile in 0.1% formic acid. The effluent

from the HPLC was directly electrosprayed into a Qexactive HF (Thermo) operated in data dependent mode to automatically switch between full scan MS and MS/MS acquisition. Survey full scan MS spectra (from m/z 250–1600) were acquired with resolution $R=60,000$ at m/z 400 (AGC target of 3×10^6). The 10 most intense peptide ions with charge states between 2 and 5 were sequentially isolated to a target value of 1×10^5 , and fragmented at 27% normalized collision energy. Typical mass spectrometric conditions were: spray voltage, 1.5 kV; no sheath and auxiliary gas flow; heated capillary temperature, 250°C; ion selection threshold, 33,000 counts. Peak integration was performed using Skyline (<https://skyline.ms/project/home/software/Skyline/begin.view>) and was further analyzed by R (R Core Team (2017). R: A language and environment for statistical computing. R Foundation for Statistical Computing, Vienna, Austria. URL <https://www.R-project.org/>).

Hematology and organ isolation

To analyze hematological parameters, blood was acquired via cardiac puncture and collected into EDTA-containing tubes (Sarstedt, Nümbrecht, Germany) and investigated using a ScilVetabc plus (Scil Animal Care Company B.V., Viernheim, Germany). Desired organs, including abdominal aorta, aortic arch, liver, lymph nodes, and spleen, were harvested with perfusion of the arterial tree with phosphate-buffered saline (Sigma Aldrich, St. Louis, USA). Organs harvested for gene expression analysis were stored in RNAlater (Life Technologies, Carlsbad, USA) for 24 hours at room temperature and afterwards frozen at -80 °C. Additionally, for flow cytometric analysis, organs were collected in phosphate-buffered saline on ice. For plaque development analysis, hearts, including the aortic root, were isolated and frozen in Tissue-Tek (Sakura, Finetek, Torrance, USA) for sectioning.

Histology and Immunohistochemistry

For plaque area quantification, 6 μm -thick serial heart sections were stained with Oil-red O (Sigma Aldrich). The brightfield images were analyzed by using an automated morphometry system (LAS 4.6 analysis, Leica Microsystems) on a Leica DM6000 microscope (Leica Microsystems, Wetzlar, Germany).

The cryosectioned aortic root slides were fixed in 100% ice-cold acetone solution before incubation with primary antibodies. The secondary antibodies (Alexa Fluor 488, Alexa-594, Cy3, Life Technologies, and Jackson ImmunoResearch, West Grove, USA) were applied to detect primary antibodies bound to the tissue samples. The counterstaining was done with hematoxylin or 4', 6' Diamidino-2-phenylindol (DAPI, Life Technologies), and DAKO fluorescent mounting medium (Dako, Agilent Technologies, Santa Clara, USA) was used. The images were taken by using a Leica DM6000 microscope. Mac3 and α -SMA positive areas were analyzed using color thresholds, whereas stained cells were counted (see Supplemental Table 3 for clones).

Gene expression

To quantify the gene expression, RNA was isolated from desired tissue samples by using the RNeasy Mini Kit II (Qiagen) and reverse transcribed with the SuperVilo cDNA synthesis kit (Life Technologies). Quantitative real-time PCR (qPCR) was performed using FAM-labelled TaqMan Assays (Applied Biosystems) and Gene Expression Master mix (Life Technologies) on a 7900HT real-time PCR system (Applied Biosystems) to analyze expression of genes (*EZH2*, *iNOS*, *Arg1*, *CD3*, *CD4*, *CD8*, *IFN γ* , *IL4*, *IL13*, *PLZF*, *Rpl13a*).

Flow cytometry

After harvesting, the lymph nodes and spleen were mashed and strained by a cell strainer (70 μ m) to prepare single cell suspension. The erythrocytes present in whole blood and spleen samples were lysed with lysis buffer (150 mM ammonium chloride (Sigma Aldrich) and 10 mM sodium bicarbonate (Sigma Aldrich), pH 7.4) for 2 minutes on ice. Then, PBS washed cells were plated in microtiter plates (Costar 3799, Corning, USA) and stained with the required antibody cocktail. To avoid nonspecific binding, cells were first treated with Fc block (anti-CD16/32, eBiosciences, clone 93, 1:100) for 20 min on ice whenever necessary. The antibody cocktail was prepared depending on experiments (see Supplementary Table 4 for clones). Intracellular staining for the transcription factors Foxp3 (FoxP3-eFluor 450, ThermoFisherScientific, clone FJK-16s, 1:40) and PLZF (PLZF APC 1: 100) were done by following manufacturer's instructions for intracellular (nuclear) proteins staining. When necessary, viability dyes (Live/Dead fixable Aqua/Violet; Life Technologies) were included in antibody panels as well. Before attaining the FACS data, fluorochrome compensation was made with UltraComp Beads (eBioscience). Single cell suspensions were investigated by using BD FACS Canto™ II (BD Biosciences) and the acquired data was analyzed with Flowjo v.10 software (Flowjo, LLC, Ashland, USA).

Cytokine measurements

Plasma and T cell supernatant cytokine levels were determined by multiplexed bead immunoassay using the Magpix instrument (Luminex, Thermo Fisher). For both specimens, T cell cytokines were analyzed using the Th1/Th2/Th9/Th17/Th22/Treg Cytokine 17-plex Mouse ProcartaPlex Panel (Thermo Fisher) according to manufacturer's instructions.

Murine single cell RNA-sequencing

Following high fat diet administration, spleens were isolated from from *Ezh2^{fl/fl}/Cd4Cre* mice after cervical dislocation. Living splenic CD45⁺CD3⁺ T cells (B220⁻Gr1⁻Ter119⁻) were sorted using a FACS Aria III (BD Biosciences) and diluted to a concentration of 1000 cells/ul per 10X genomics protocol. Single cell libraries were generated using the Chromium Next GEM Single Cell 3' Reagent Kit v3.1 (10x Genomics, Pleasanton, CA). Sequencing of the 10x Chromium gene expression library was performed on an Illumina HiSeq 1500 instrument with 28 bases read 1 and 50 bases read 2 and an 8 bases index read. Raw data was demultiplexed based on the i7 index sequences using deML⁵⁸. Next the fastq files were quality filtered, mapped and converted into a count table using the zUMIs pipeline (version 2.9.4d)⁵⁹. Mapping to the GRCm38 genome was performed using STAR (version 2.6)⁶⁰ with Gencode vM25 gene annotation. To distinguish small cells from truly empty droplets, cellbender⁶¹ was used, and the final count matrix was subset for the identified barcodes. scRNA-seq analysis was then performed in RStudio (Version 1.3.1093) using the Seurat package (version 4.0.2)²³. Separate Seurat objects were created for wild-type and knockout reads, and genes were excluded if expressed in fewer than 30 cells. Merge() was used to combine the wild-type and knockout datasets. SCTransform normalization²⁴ was adopted to mitigate the possible sources of variations like cell cycle as well as technique-related influence. The Uniform Manifold Approximation and Projection (UMAP) was used to convert cells into a two dimensional map.

Bulk RNA-sequencing

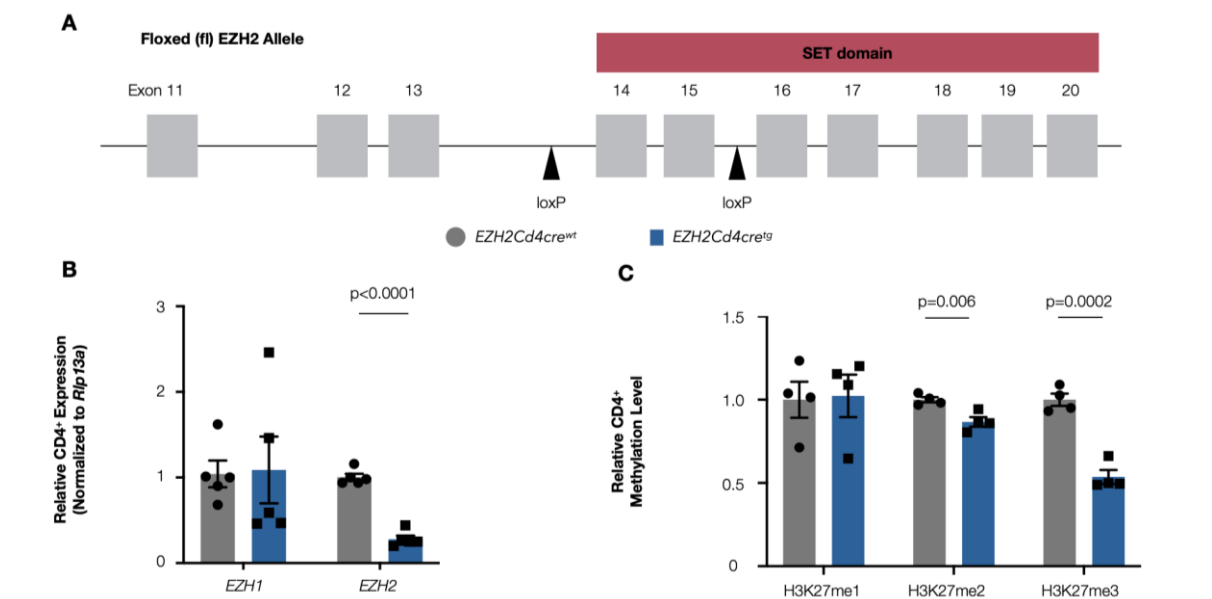
The harvested lymph nodes and spleen were processed with forceps and filtered through a 70 µm strainer to prepare single-cell suspensions. Spleen Erythrocytes were lysed for 2 minutes on ice with an erylysis buffer consisting of 150 mM Ammonium chloride (Sigma Aldrich) and 10 mM Sodium bicarbonate (Sigma Aldrich) at pH= 7.4. CD4⁺ T

cells were isolated from the prepared cell suspensions using antibody-conjugated magnetic beads according to the manufacturer's instructions (Dynabeads Untouched Mouse CD4, Life Technologies). For bulk RNA sequencing, RNA was isolated from approximately 1 million CD4⁺ T cells by following the manufacturer protocol of the RNeasy kit (Qiagen). Subsequently, the cDNAs, library preparation, and data analysis were done using an adapted version of prime-seq (step by step protocol: <https://www.protocols.io/view/prime-seq-s9veh66>) described previously.

Briefly, extracted RNA was DNase I treated and then reverse transcribed into full-length cDNA using barcoded oligodT primers and template switching oligos. Following first strand synthesis, the samples were pooled, cleaned with magnetic beads, and remaining primers were digested using Exonuclease I. Second strand synthesis and pre-amplification was performed, and the amplified cDNA was quantified using PicoGreen and qualified using a HS DNA chip on the Bioanalyzer (Agilent). High quality samples were used for library construction using the NEB Next Ultra II FS kit (NEB) according to prime-seq specifications. The libraries were quantified and qualified using the HS DNA chip on the Bioanalyzer (Agilent) and then sequenced using a Hiseq 1500 with the following parameters: R1: 28, i7: 8, R2: 50 cycles.

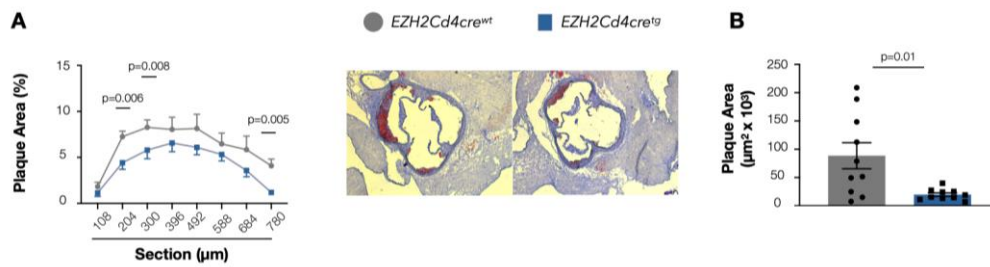
The raw data was pre-processed with zUMIs (version 2.5.5)⁵⁹, including filtering, mapping to the mouse genome (GRCm38.85), and counting. Differential gene expression analysis was performed using the DEseq2⁶² bioconductor package in an R environment (3.5.3) and functional annotation of differentially expressed genes was done with Qiagen Ingenuity Pathway Analysis (data content version 49932394)⁶³.

Supplemental Figures and Figure Legends



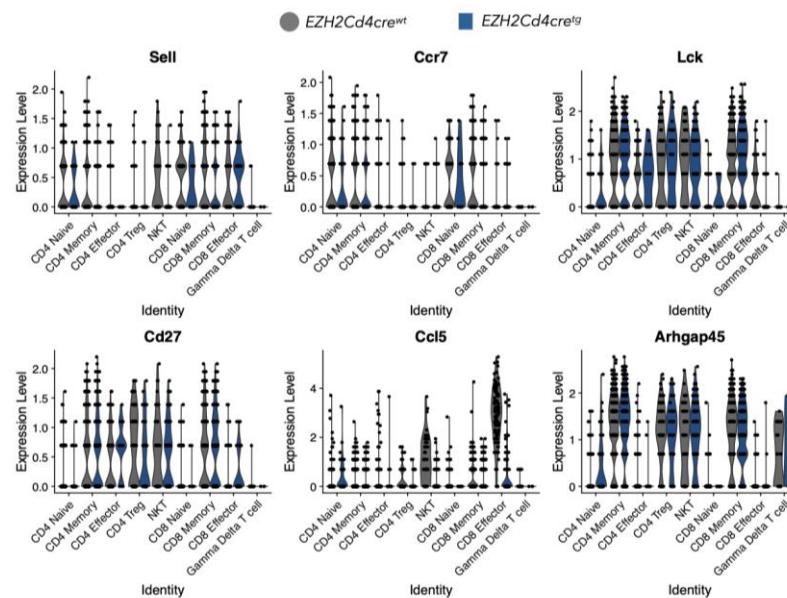
Supplemental Figure 1 Conditional EZH2 knockout model generation and confirmation for *Ezh2^{fl/fl}/Cd4Cre* mice

A, Model for insertion of loxP sites into the EZH2 gene flanking exon 14 and 15, which partially code for the methyltransferase activity-conferring SET domain. Floxed exons can be excised by cre-mediated recombinase. **B-C**, Confirmation of *Ezh2^{fl/fl}/Cd4Cre* model using **(B)** qPCR to analyze gene expression of both *EZH1* and *EZH2* (n=5) from *in vitro* concanavalin A activated CD4⁺ T cells and **(C)** mass spectrometry of histone modifications including histone 3 lysine 27 monomethylation (H3K27me1), histone 3 lysine 27 dimethylation (H3K27me2), and histone 3 lysine 27 trimethylation (H3K27me3) isolated directly from splenic CD4⁺ T cells (n=4). Data are all represented as mean \pm s.e.m. and analyzed using a two-tailed Student's *t* test.



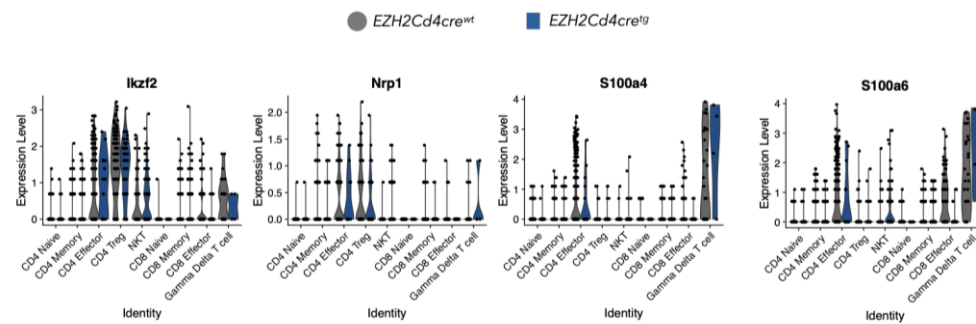
Supplemental Figure 2 T-cell specific EZH2 deficiency reduces plaque burden in male mice in both the aortic root and aortic arch

A, Atherosclerotic plaque area (%) across the aortic root in male *Ezh2^{fl/fl}/Cd4Cre* mice (n=10) at the indicated positions (left) with representative Oil Red O-stained images (right). **B**, Atherosclerotic plaque area from the aortic arch in male *Ezh2^{fl/fl}/Cd4Cre* mice (n=10). Data are all represented as mean \pm s.e.m. and analyzed using either a two-tailed Student's *t* test (**A**) or two-tailed Mann-Whitney test (**B**).



Supplemental Figure 3 Feature plots to identify naïve and effector T cell populations from single cell RNA-sequencing of splenic CD3⁺ from *Ezh2^{fl/fl}/Cd4Cre* mice

Feature plots displaying expression levels for *Sell*, *Ccr7*, *Lck*, and *Cd27* to help identify naïve, memory, and effector T cell populations. Feature plot displaying expression levels for *Ccl5* to help identify CD8 effector T cells. Feature plot displaying expression levels for *Arhgap45* to help distinguish memory and effector T cells. Expression profiles are split between *Ezh2^{fl/fl}/Cd4Cre^{tg}* mice (blue) and their wild-type littermates (grey) per cluster.



Supplemental Figure 4 Feature plots to identify Treg and effector T cell populations

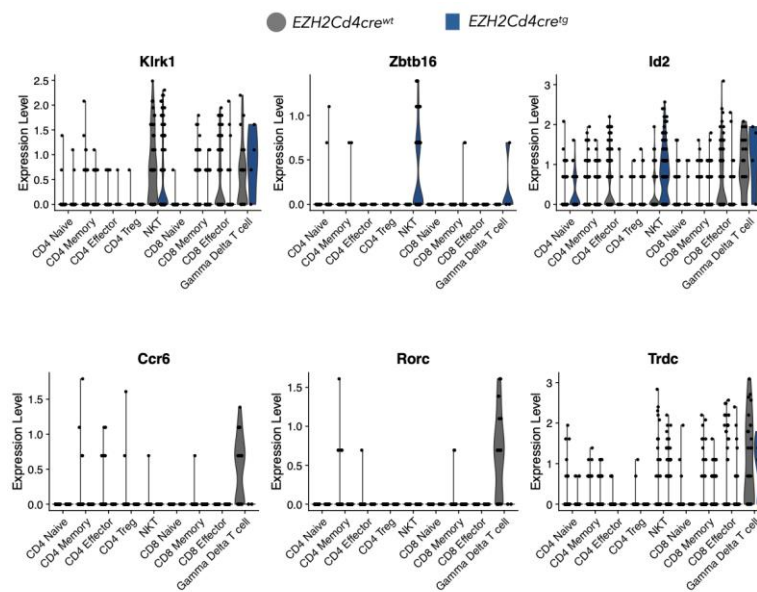
from single cell RNA-sequencing of splenic CD3⁺ from *Ezh2^{fl/fl}/Cd4Cre* mice

Feature plots displaying expression levels for *Ikzf2* and *Nrp1* to help identify T regula-

tory (Treg) cells. Feature plot displaying expression levels for *S100a4* and *S100a6* to

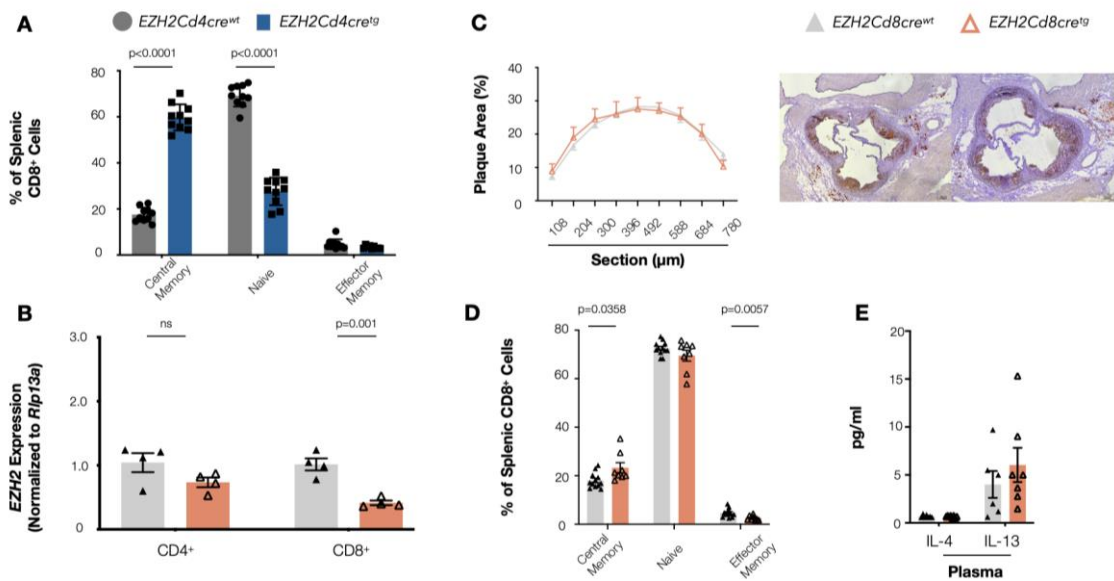
help distinguish effector T cells from Tregs. Expression profiles are split between

Ezh2^{fl/fl}/Cd4Cre^{tg} mice (blue) and their wild-type littermates (grey) per cluster.



Supplemental Figure 5 Feature plots to identify NKT and $\gamma\delta$ T cell populations from single cell RNA-sequencing of splenic CD3⁺ from *Ezh2^{fl/fl}/Cd4Cre* mice

Feature plots displaying expression levels for *Klrk1*, *Zbtb16*, *Id2* to help identify natural killer T (NKT) cells. Feature plot displaying expression levels for *Ccr6*, *Rorc*, and *Trdc* to help distinguish gamma-delta ($\gamma\delta$) T cell from NKT cells. Expression profiles are split between *Ezh2^{fl/fl}/Cd4Cre^{tg}* mice (blue) and their wild-type littermates (grey) per cluster.



Supplemental Figure 6 CD8-specific EZH2 deficiency does not affect atherosclerosis or production of type II cytokines

A, Flow cytometric analysis of CD8⁺ populations in *Ezh2^{fl/fl}/Cd4Cre* mice (n=10). **B**, Gene expression analysis using qPCR to compare *Ezh2* in concanavalin A activated CD4⁺ and CD8⁺ T cells from mice with a CD8-specific EZH2 deficiency (*Ezh2^{fl/fl}/Cd8Cre^{tg}*) and their wildtype littermates (n=4). **C**, Atherosclerotic plaque area (%) across the aortic root in male *Ezh2^{fl/fl}/Cd8Cre* mice (n=10-13) at the indicated positions (left) with representative Oil Red O-stained images (right). **D**, Flow cytometric analysis of CD8⁺ populations in *Ezh2^{fl/fl}/Cd8Cre* mice (n=8-12). **E**, Multiplexed cytokine measurements for IL-4 and IL-13 in the plasma of *Ezh2^{fl/fl}/Cd8Cre* mice (n=6-8). Data are all represented as mean \pm s.e.m. and analyzed using either a two-tailed Student's *t* test (**A**, **B**, **C**, **D**: naïve, effector memory, **E**) or two-tailed Mann-Whitney test (**D**: central memory).

Supplemental Tables

Parameter	EZH2Cd4cre ^{wt}	EZH2Cd4cre ^{tg}	p-value
Weight (g)	26.48 ± 1.41	25.10 ± 0.94	0.68
VLDL (mM)	3.14 ± 0.02	2.76 ± 0.13	0.19
LDL (mM)	4.56 ± 0.38	3.96 ± 0.18	0.18
HDL (mM)	0.47 ± 0.03	0.57 ± 0.05	0.14
White Blood Cells (10 ³ /μL)	2.57 ± 0.14	2.44 ± 0.24	0.64
Lymphocytes (10 ³ /μL)	1.73 ± 0.13	1.56 ± 0.14	0.42
Monocytes (10 ³ /μL)	0.10 ± 0.01	0.11 ± 0.02	0.59
Granulocytes (10 ³ /μL)	0.74 ± 0.06	0.75 ± 0.09	0.99
Red Blood Cells (10 ⁶ /μL)	9.02 ± 0.11	8.89 ± 0.13	0.46
Hemoglobin (mmol/L)	8.99 ± 0.08	8.70 ± 0.13	0.08
MCH (fmol)	0.99 ± 0.01	0.98 ± 0.01	0.17
MCHC (mmol/L)	19.06 ± 0.09	19.06 ± 0.10	0.98
MCV (fl)	52.00 ± 0.36	51.42 ± 0.48	0.21
Platelets (10 ³ /μL)	877.70 ± 21.95	972.60 ± 48.26	0.48

Supplemental Table 1 14 parameters were compared between *Ezh2^{fl/fl}/Cd4Cre^{tg}* mice and their wild-type littermates as confirmation of minimal negative consequences from EZH2 knockout. Data are all represented as mean ± s.d.

Parameter	EZH2Cd8cre ^{wt}	EZH2Cd8cre ^{tg}	p-value
Weight (g)	25.39 ± 2.20	24.11 ± 1.14	0.11
VLDL (mM)	1.69 ± 0.19	1.45 ± 0.53	0.37
LDL (mM)	4.12 ± 0.89	3.19 ± 0.52	0.07
HDL (mM)	0.55 ± 0.04	0.49 ± 0.13	0.36
White Blood Cells (10 ³ /μL)	2.34 ± 0.45	2.57 ± 0.50	0.27
Lymphocytes (10 ³ /μL)	1.63 ± 0.38	1.81 ± 0.43	0.32
Monocytes (10 ³ /μL)	0.06 ± 0.05	0.07 ± 0.05	0.59
Granulocytes (10 ³ /μL)	0.65 ± 0.13	0.69 ± 0.12	0.47
Red Blood Cells (10 ⁶ /μL)	9.37 ± 0.37	9.24 ± 0.54	0.53
Hemoglobin (mmol/L)	9.08 ± 0.39	8.91 ± 0.46	0.44
MCH (fmol)	0.98 ± 0.04	0.97 ± 0.04	0.58
MCHC (mmol/L)	18.66 ± 0.50	18.77 ± 0.72	0.73
MCV (fl)	52.00 ± 1.21	51.70 ± 1.64	0.63
Platelets (10 ³ /μL)	937.1 ± 88.28	913.5 ± 97.03	0.56

Supplemental Table 2 14 parameters were compared between *Ezh2^{fl/fl}/Cd8Cre^{tg}* mice and their wild-type littermates as confirmation of minimal negative consequences from EZH2 knockout. Data are all represented as mean ± s.d.

Antibody	Company	Clone	Dilution
Mac3	BD Biosciences	M3/84	1:200
Alpha smooth muscle actin (α-SMA)	Sigma Aldrich	1A4	1:1000
CD3	BD Biosciences	145-2C11	1:100
CD4	BD Biosciences	RM4-5	1:100
iNOS	Cell Signaling	145-2C11	1:100
Arg1	Cell Signaling	D4E3M	1:50

Supplemental Table 3 Immunohistochemical antibodies used in the present study.

Antibody	Company	Clone	Dilution
CD45 PB/PerCP	Biologend	30F11	1:1000
CD11b PerCP	eBioscience	M1/70	1:500
CD19 Pe-Cy7	eBioscience	eBio1D3	1:500
CD3 FItc	eBioscience	145-2C11	1:200
CD115 APC	Biologend	AFS98	1:500
Ly6C BV510	Biologend	HK1.4	1:500
Ly6G PE	BD Biosciences	1A8	1:2000
CD4 BV510	Biologend	RM4-5	1:1000
CD44 APC	eBiosciences	IM7	1:500
CD62L APC-Cy7	Biologend	MEL-14	1:1000
CD25 PE	eBiosciences	PC61.5	1:300
Foxp3 PB	eBiosciences	FJK-16s	1:40
CXCR3 PE-Cy7	Biologend	CXCR3 PE-Cy7	1:100
CCR6 PE	Biologend	29-2L17	1:100
CD1d PBS-57 PB	NIH Tetramer Core Facility	-	1:500
CD8 PE/PerCP	eBiosciences	53-6.7	1:200
TCRb APC-H7	Invitrogen	H57-597	1:100
PLZF APC	BD Bioscience	R17-809	1:100

Supplemental Table 4 Flow cytometry antibodies used in the present study.

Acknowledgements

It's hard to believe that I'm closing in on the end of my time as a PhD student. Almost six years ago, I made the decision to move across the Atlantic for what I thought would just be a two-year journey starting as a lab technician. I would have never guessed all of the opportunities that have been presented to me once I moved to Germany. During the past few years, both my personal and professional life has grown tremendously. I have been incredibly lucky to have wonderful friends, family, and coworkers who have supported me every step of the way. Therefore, I would like to sincerely thank all of the people who have made this journey possible.

First and foremost, I would like to thank Prof. Christian Weber who has been instrumental in all of my projects during my time at IPEK. I greatly appreciate both your financial and personal support throughout my career. Your scientific advice and expertise was crucial for moving many of my projects forward.

A very special thanks to Prof. Jürgen Bernhagen for giving me the chance to start my scientific career in Germany. I was incredibly nervous to move to a new country, but your lab welcomed me with open arms. I enjoyed my time in Großhadern helping start your new lab and learning the secrets of MIF purification. Even after my time in your lab, together you and Prof. Axel Imhof have been wonderful mentors advising me in my current projects. My time with both you and Omar was invaluable in shaping a lot of my scientific fundamentals.

I would also like to give a special thanks to Prof. Sabine Steffens for her organization of the IRTG1123 graduate school. I really appreciate all of your help in transversing the sometimes confusing waters of graduate school in Germany. With the support of the graduate school, I was able to gain invaluable feedback and networking opportunities that helped shape my PhD.

I can't even think of a way to express all of the gratitude I have for my two mentors, Dr. Dorothee Atzler and Prof. Esther Lutgens.

Dear Doro, It's crazy seeing how far we've come now and thinking about when we first met, and you would have to listen to all of my crazy life details together with Omar in the Großhadern cantina. Thank you for pushing me to pursue the PhD in the first place. Before starting at IPEK, I was on the fence and nervous about what might happen, but you've

made this an unforgettable experience. Thank you for constantly pushing me throughout the PhD to make the experience the best it could be. But also thank you for being there when I needed an outlet for venting some frustration that I had in the lab no matter how large or small the problem might have been. You've been a wonderful mentor and friend. I'm very excited to see what the future brings and hope we can keep the same close connection.

Dear Esther, thank you for all of your support both financially and personally over the past few years. Whenever I was stuck in my project, I knew I could always talk with you about it (either in person or over Zoom) and you would have some insight that I would have never thought about. What made my time in your lab even more special was your consistent positive attitude. It was a joy to meet and discuss science with you because you were always just as excited for my results as I was. But you also were incredibly understanding during the failures, which was a nice feeling as a young scientist. I'm excited to see what happens with your move to the US, and perhaps one day we can navigate the US research system together.

Without both of your support, Doro and Esther, I know my understanding of science as well networking would not be where it is today. You both have supported me in all aspects of my career, and I know I am a better scientist because I worked with you. Thank you for all of the opportunities you have given me.

Liebe Sigrid, in den letzten vier Jahren hast du mir immer gesagt, dass ich Deutsch sprechen muss, um meinen Abschluss zu machen, also dachte ich, du würdest dich freuen, wenn deine Nachricht auf Deutsch wäre. Obwohl meine Grammatik wahrscheinlich schrecklich ist :) Danke, dass du so ein toller Freund und Mitarbeiter während meiner Zeit bei IPEK warst. Ich glaube nicht, dass ich meine Promotion ohne all deine Hilfe während der Experimente und harvests überlebt hätte. Aber was noch wichtiger ist, ich glaube nicht, dass ich ohne dich überlebt hätte, mit dem ich jeden Tag quatschen konnte. Und der Prosecco am Freitagnachmittag und die Grillabende haben auch geholfen!

Liebe Sabine, ich könnte versuchen, Dir auch auf Deutsch zu schreiben, but you know how terrible my German is :) Thank you for always being there to discuss everything from politics to German life. Although we're no longer in the garden pavilion, I always enjoy stopping by to chat with you still. Thanks for always being a good friend and coworker.

My time at IPEK would also not be the same without the great group members we have had both past and present. Thanks to Carina for helping me in the beginning to get settled in at IPEK. A very special thanks to Tobi who made the GP a great place to work. Forcing me to speak German and stay late at GP get togethers. Thanks to Yuting and Katrin for all of their help and support over the past few years with all of my experiments. Although they only started a few months, a special thanks for Cecilia and Roberta (and Floriana) for making the move to the basement feel like home. Especially thanks to Cecilia for being so flexible and adaptable to the different experiments that we have to work on with the EZH2 project. Thanks to Mahadia and Abbie for all of your support with my projects especially when my experimental planning was not always the best. And thanks to Yonara for all of your support for IHC protocols.

I would also like to thank all of the GP people, especially Xavier, Rundan, Julian, Lusi, Philipp, Michael, Shu, Yuanfang, and Chuankai for making my time there wonderful. Xavier, in particular, thanks for always being there to discuss my results and advise me on where to go next. But also understanding my sarcasm and responding with your own :)

In addition, I would like to thank all of the people from the greater IPEK family. Special thanks to Yvonne Jansen for being a super technician who can literally do anything. Thanks to Remco for all of his help with microscopy and Johan for his help with the FACs. To Sarah, Emiel, Selin, Linsey, Yanni, Pati, Sanne, Carolin, Lucia, Georg, Saffiyeh, Ting, Mariaelvy, and Donato thanks for all of your help and enjoyable moments.

Before starting my PhD, I had multiple advisors who provided me with invaluable feedback and opportunities during each step of the way. Thanks to Prof. Jung-Bum Shin, Dr. Josh Katz, and Dr. Emily Hill.

I owe one of my greatest thanks for my family who have pushed me to reach my goals since before I can remember. To my parents, Belinda and Barry, who always believed in me and showed me the value of hardwork. To my sister and brother-in-law, Kelly and Chanon, who was always one of my biggest cheerleaders throughout life. To my parents-in-law, Vesna and Nikola, who showed me that you could do great things no matter where you live. To my nieces, Kennedy and Madison, who always brightened my day. Thank you all for your unconditional support even if you weren't initially happy with the move to Germany. Your words of encouragement meant the world to me when things weren't

progressing the way I would like during my career. Thank you all for the thousands of FaceTime calls and visits between the US and Germany to help get me to end of the PhD. Finally, my biggest thank you goes to my husband, Aleks. I remember when we met during our bachelors and we both talked about one day finishing our PhDs. Now, we've both accomplished that together. I never imagined that our PhDs would be so intertwined, but you've been my biggest collaborator even if you weren't always happy about making my cDNA libraries. Thanks for always being there for me to discuss my successes and failures. I think it's incredibly rare that two people are able to share such a great life together, but also be involved in each other's professional lives as well. Whenever something was going wrong, I could always count on you to either be a text away or waiting at home to tell me things weren't as bad as I thought. But also thanks for pushing to live outside my comfort zone. Our life has been a lot of you getting me to try new foods or explore new places, and I think it's helped me become a better person. I can't wait to see what the next chapter holds for us.